Journal Pre-proof

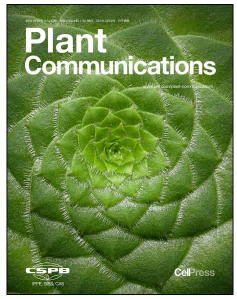

A predictive model for ethylene-mediated auxin and cytokinin patterning in the *Arabidopsis* root

Simon Moore, George Jervis, Jennifer F. Topping, Chunli Chen, Junli Liu, Keith Lindsey

PII: S2590-3462(24)00128-7

DOI: https://doi.org/10.1016/j.xplc.2024.100886

Reference: XPLC 100886

To appear in: *PLANT COMMUNICATIONS*

Received Date: 10 October 2023

Revised Date: 25 February 2024

Accepted Date: 18 March 2024

Please cite this article as: Moore, S., Jervis, G., Topping, J.F., Chen, C., Liu, J., Lindsey, K., A predictive model for ethylene-mediated auxin and cytokinin patterning in the *Arabidopsis* root, *PLANT COMMUNICATIONS* (2024), doi: https://doi.org/10.1016/j.xplc.2024.100886.

This is a PDF file of an article that has undergone enhancements after acceptance, such as the addition of a cover page and metadata, and formatting for readability, but it is not yet the definitive version of record. This version will undergo additional copyediting, typesetting and review before it is published in its final form, but we are providing this version to give early visibility of the article. Please note that, during the production process, errors may be discovered which could affect the content, and all legal disclaimers that apply to the journal pertain.

© 2024

A predictive model for ethylene-mediated auxin and cytokinin patterning in the *Arabidopsis* root

Simon Moore[1,2], George Jervis[1], Jennifer F. Topping[1], Chunli Chen[2,3], Junli Liu[1*], and Keith Lindsey[1*]

[1]Department of Biosciences, Durham University, South Road, Durham DH1 3LE, UK

[2]Hubei Hongshan Laboratory, College of Life Science and Technology, Huazhong Agricultural University, Wuhan 430070, China

[3]National Key Laboratory for Germplasm Innovation and Utilization for Fruit and Vegetable Horticultural Crops, Huazhong Agricultural University, Wuhan, Hubei 430070, China

*Joint corresponding authors

Correspondence: Keith Lindsey (keith.lindsey@durham.ac.uk), Junli Liu (junli.liu@durham.ac.uk)

Running title: Modelling simultaneous hormone patterns

Short summary:

We utilize a wide range of experimental observations to propose a mechanism for simultaneous patterning of auxin and cytokinin concentrations. The mechanism reveals that ethylene signalling is an important factor in achieving simultaneous auxin and cytokinin patterning, while also predicting other experimental observations. This research reveals the importance of hormonal crosstalk in patterning auxin, cytokinin and ethylene in the *Arabidopsis* root.

ABSTRACT

The interaction between auxin and cytokinin is important in many aspects of plant development. Experimental measurements of both auxin and cytokinin concentration and reporter gene expression clearly show the coexistence of auxin and cytokinin concentration patterning in *Arabidopsis* root development. However, in the context of crosstalk between auxin, cytokinin and ethylene, little is known about how auxin and cytokinin concentration patterns simultaneously emerge and how they regulate each other in the *Arabidopsis* root. This work utilizes a wide range of experimental observations to propose a mechanism for simultaneous patterning of auxin and cytokinin concentration. In addition to the regulatory relationships between auxin and cytokinin, the mechanism reveals that ethylene signalling is an important factor in achieving simultaneous auxin and cytokinin patterning, while also predicting other experimental observations. Combining the mechanism with a realistic *in silico* root model reproduces experimental observations of both auxin and cytokinin patterning. Predictions made by the mechanism can be compared with a variety of experimental observations, including those conducted by our group and other independent experiments reported by other groups. Examples of these predictions include patterning of auxin biosynthesis rate, PIN1 and PIN2 pattern changes in *pin3, 4, 7* mutants, cytokinin patterning change in the *pls* mutant, PLS patterning, as well as various trends in different mutants. This research unravels a plausible mechanism for simultaneous patterning of auxin and cytokinin concentrations in *Arabidopsis* root development and suggests a key role for ethylene pattern integration.

Key words: *Arabidopsis* root, auxin patterning, cytokinin patterning, ethylene signalling, *in silico* digital root, spatiotemporal modelling.

INTRODUCTION

A major challenge in plant developmental biology is understanding how development is coordinated by interacting hormones and genes. Plant hormones (Santner and Estelle, 2009) can act antagonistically or synergistically to regulate cell proliferation, elongation and differentiation (Garay-Arroyo et al., 2012; Vanstraelen and Benkova, 2012). The importance of the interaction between auxin and cytokinin in root and shoot development and the maintenance of cell proliferation was shown in very early experiments on cultured tobacco callus (Skoog and Miller, 1957) where the ratio of cytokinin to auxin determined the developmental pathway. While all hormones are involved in the regulation of root development, auxin and cytokinin play central roles in regulating the size of the meristem and root growth (Chandler and Werr 2015; Perilli et al., 2012; Schaller et al., 2015; Friml 2021; Roychoudhry and Kepinski 2022).

Auxin and cytokinin cellular concentrations are a function of multiple factors including biosynthesis (Ljung 2013; Jones and Ljung 2011; Zhao 2010; 2014; Casanova-Sáez et al. 2021), degradation (Jones and Ljung 2011; Ljung 2013; Casanova-Sáez et al. 2021) and conjugation (Ludwig-Muller 2011). Importantly, both auxin and cytokinin concentrations display distinct patterns in the *Arabidopsis* root. Measuring auxin concentration revealed the presence of IAA concentration gradients within the *Arabidopsis* root tip with a distinct maximum in the organizing quiescent centre (QC) of the root apex (Petersson et al., 2009). Measuring cytokinin concentration revealed an intercellular cytokinin gradient in the primary root tip, with maximum levels in the lateral root cap, columella, columella initials, and QC cells (Antoniadi et al., 2015). Thus, these experimental data directly show that auxin and cytokinin concentration patterns coexist in the *Arabidopsis* root.

Many reporter gene expression studies for both auxin and cytokinin are also consistent with the existence of auxin and cytokinin gradients in *Arabidopsis* root (Isoda et al. 2021; Jedlickova et al. 2022). Response patterning, generated by reporter constructs based on various naturally occurring and synthetic promoters, includes imaging of *IAA2::GUS* and *DR5::GFP* (Grieniesen et al., 2007), *DII-VENUS* (Brunoud et al., 2012) and *R2D2* (Liao et al., 2015) for auxin, and *ARR5::GUS* (Werner et al., 2003) and *TCSn::GFP* (Zurcher et al., 2013) for cytokinin. Since the relationship between hormone concentration and the expression of a reporter gene can be non-linear, patterning of reporter gene expression can differ from concentration patterning. Moreover, expression patterning can vary between different response reporters, since, in addition to hormone concentrations, reporter response patterning also depends on other factors such as the sensitivity of the reporter promoter to a hormone. Moreover, reporter expression can also be influenced by multiple signalling pathways as shown in Liu et al. (2017). Nevertheless, patterning of reporter gene expression for both auxin and cytokinin has been widely accepted as a proxy for auxin and cytokinin concentration patterns.

Measurements of both auxin and cytokinin concentration and reporter gene expression clearly show the coexistence of auxin and cytokinin concentration patterning in *Arabidopsis* root development (Petersson et al., 2009; Antoniadi et al., 2015; Grieniesen et al., 2007; Liao et al., 2015; Brunoud et al., 2012; Werner et al., 2003; Zurcher et al., 2013). Moreover, a wide range of experimental data show that auxin, cytokinin and ethylene form a complex crosstalk network. Despite progress in experimental studies little is known about how auxin and cytokinin concentration patterns simultaneously emerge and how they regulate each other in the *Arabidopsis* root in the context of crosstalk between auxin, cytokinin and ethylene. Importantly, although various experimental data accumulated over many years have indicated that both auxin and cytokinin patterning play central roles in root development (Chandler and Werr 2015; Perilli et al. 2012; Schaller et al. 2015), an experimentally based mechanism for simultaneous auxin and cytokinin patterning is still elusive. For example: what is the mechanism for the emergence of auxin biosynthesis rate patterning, as experimentally measured in Petersson et al. (2009); what is the mechanism for PIN1 and PIN2 patterning changes in a variety of *pin* mutants, as observed by Blilou et al. (2005) and Omelyanchuk et al. (2016); and what is the mechanism for changes in cytokinin patterning in the *pls* mutant reported by Casson et al. (2002)? Therefore, to further elucidate the mechanisms that drive root development, it is essential to better understand the complex multiple relationships between auxin and cytokinin and other developmentally critical hormones, proteins and processes.

Auxin fluxes in the *Arabidopsis* root can be described by reverse fountain models (Petrasek and Friml, 2009). Auxin influx and efflux transporters play a key role in auxin patterning (Petrasek and Friml, 2009). Auxin patterning in the *Arabidopsis* root has been subjected to extensive research, in particular, by combining experimental and modelling research (Grieneisen et al. 2007; Band et al. 2014; Moore et al. 2015; 2017; Rutten et al. 2022). Moreover, crosstalk between auxin and cytokinin has also been subjected to combined experimental and modelling studies. For example, Muraro et al. (2011; 2013; 2016) have studied how cytokinin affects auxin-regulated gene expression and how meristem size is regulated by both auxin and cytokinin. Modelling of auxin and cytokinin crosstalk has also been used to elucidate root vascular patterning (Muraro et al. 2014; De Rybel et al. 2014; el-Showk et al. 2015; Mellor et al. 2017; Mellor et al. 2019; Bagdassarian et al. 2023). In addition, how complex auxin and cytokinin hormonal crosstalk regulates cell-fate specification has also been modelled (Garcia-Gomez et al. 2017; 2020). However, in the context of crosstalk between auxin, cytokinin and ethylene, little is known about how auxin and cytokinin concentration patterns regulate each other in the *Arabidopsis* root. We previously showed that, although auxin patterns can be correctly generated by integrating a hormonal crosstalk network with auxin transporters (Moore et al. 2015; 2017), the modelled cytokinin patterns are not in agreement with experimental observations (Moore et al. 2015; Liu et al. 2017). In this work, we propose an integrative mechanism for the simultaneous patterning of both auxin and cytokinin in the *Arabidopsis* root, based on a wide range of experimental data in the literature. The mechanism for simultaneous auxin and cytokinin patterning in *Arabidopsis* root is unravelled by integrating a range of experimental data and is validated by both our experimental data (such as PLS protein patterning and cytokinin response patterning changes in *pls* mutant), and independent experimental data (such as patterning of the rate of auxin biosynthesis and PIN1 and PIN2 protein patterning changes in *pin3, pin4, pin7* and *pin3,4,7* mutants).

RESULTS

Interrogating and integrating biological knowledge to form an integrative mechanism for the simultaneous patterning of auxin and cytokinin in the *Arabidopsis* root

In developing a model to explain how auxin and cytokinin patterning can be generated, we first looked at relevant evidence from experimental studies. Nordstrom et al. (2004) proposed that auxin inhibits cytokinin biosynthesis and that cytokinin inhibits auxin biosynthesis in the whole seedling. Results indicated that different types of cytokinin (iP and Z type) were predominantly synthesised in either the shoot (Z) or the root (iP) and that while biosynthesis of the Z type cytokinin was inhibited by auxin, the biosynthesis of iP type cytokinin was not inhibited and even potentially promoted by the application of auxin. Therefore, an additional conclusion from this paper could be that while auxin inhibits cytokinin biosynthesis in the whole plant, it might not inhibit cytokinin biosynthesis in the root and could possibly promote it.

Additional studies suggest that cytokinin promotes auxin biosynthesis (Jones et al., 2010), auxin upregulates cytokinin biosynthesis through *SHY2* and *IPT5* genes (Dello Ioio et al., 2008), and auxin promotes cytokinin biosynthesis through TM05 and LOG4 (De Rybel et al., 2014). Jones et al. (2010) concluded that cytokinin promotes auxin biosynthesis in young

Journal Pre-proof

developing tissues and that cytokinin inhibits its own biosynthesis through the induction of cytokinin oxidases.

Cytokinin concentrations are determined by the balance between biosynthesis, degradation, and transport. Biosynthesis is regulated by rate limiting steps involving the IPT group of enzymes, while irreversible cytokinin degradation occurs through the action of a set of cytokinin oxidases (Werner et al., 2003, 2006). Cytokinin signalling acts through receptors at the plasma membrane and the endoplasmic reticulum (ER) and then through a phospho-relay cascade to activate a set of Type-B ARR transcription factors that target the Type-A ARRs which, while not transcription factors, act as inhibitors of Type-B ARRs (To et al., 2007). Therefore, within this initial pathway cytokinin limits its own responses. Cytokinin is also self-regulated by the activity of cytokinin oxidase (CKX) where increased cytokinin treatment initially increases CKX activity and then reduces it (Figure 4 in Chatfield and Armstrong, 1986).

A Type-B ARR of particular interest is ARR2 which appears to have unique properties, whereby phosphorylated ARR2 is rapidly degraded by the proteasome while other Type-B ARRs are not (Kim et al., 2012). Non-degradable ARR2 was found to increase cytokinin sensitivity and to upregulate Type-A ARRs. Multiple ARR2 binding motifs found in the promoter regions of cytokinin-induced genes have led to the suggestion that ARR2 could act as a master regulator of cytokinin signalling responses (Hwang and Sheen, 2001).

ARR2 also links the cytokinin pathway with the ethylene pathway (Hass et al., 2004). ARR2 binds the *ERF1* promoter and upregulates *ERF1* expression. A stabilized phosphorylated (active) ARR2 showed an ethylene response in the absence of ethylene, even in the presence of AVG, an inhibitor of ethylene biosynthesis. Furthermore, the *arr2* null mutant has a reduced ethylene response, which is rescued by expressing *ARR2* under the control of the *35S* promoter. There are also links in the opposite direction from the ethylene pathway to the cytokinin pathway (Hass et al., 2004) via ARR2. The ethylene receptor ETR1 appears to phosphorylate ARR2 since the ethylene sensitive *etr1-7* (Cancel and Larsen, 2002) loss-of-function mutant (low receptor activity and high downstream ethylene signalling) has reduced levels of phosphorylated ARR2 (Hass et al., 2004). It was concluded that an ETR1-dependent phospho-relay regulates ARR2 phosphorylation and activity (Hass et al., 2004). An additional link between the ethylene and cytokinin pathways is that EIN3 inhibits *ARR5*, a Type-A ARR commonly used in cytokinin reporter constructs (El-Showk et al., 2013; Shi et al., 2012).

There are also multiple links between the cytokinin and auxin pathways. Auxin upregulates *IPT* genes through SHY2 (Dello Ioio et al., 2008; Kushwah et al., 2011), and Type-B ARRs

ARR1 and ARR12 in turn promote *SHY2* (Dello Ioio et al., 2008; El-Showk et al., 2013), which inhibits *ARF* in the auxin signalling pathway. Auxin also promotes the transcription of *AHP6*, an inhibitor of cytokinin signalling response (Bishopp et al., 2011).

ARR2 is suggested to be a central Type-B ARR within the cytokinin signalling pathway, with links to and from the ethylene pathway. Microarray analysis indicates that ARR2 promotes *CKX* expression and activity since *CKX* mRNA is reduced by 2.9 fold in the *arr2* null mutant and increased by 14.1 fold with stabilized activated ARR2, which cannot be degraded and mimics phosphorylation (Hass et al., 2004). Therefore, activity of the ethylene receptor ETR1 appears to be able to regulate cytokinin concentrations and response through ARR2 and CKX, by phosphorylating ARR2 and increasing its activity (Hass et al., 2004). As such, it is proposed that active ETR1 receptors (in the absence of ethylene) result in ARR2 phosphorylation and increased ARR2 activity, which in turn results in increased CKX activity and reduced cytokinin. In the presence of ethylene, ETR1 activity is reduced which decreases ARR2 phosphorylation and activity and so reduces CKX activity and increases cytokinin concentrations. This is consistent with experimental results which show an increase in cytokinin concentration in the ethylene hyper-signalling *pls* mutant compared to wildtype (Liu et al., 2010).

These lines of evidence indicate that ethylene responses positively regulate cytokinin concentration by inhibiting CKX activity. In previous studies on auxin, cytokinin and ethylene crosstalk in the *Arabidopsis* root (Liu et al., 2010, 2013; Moore et al., 2015, 2017), the regulation of cytokinin concentration by ethylene signalling was not studied. In previous work (Moore et al., 2015), even after cytokinin biosynthesis was restricted to the vascular cylinder, the modelled cytokinin patterning was still significantly different from experimental observations (Werner et al., 2003). Previous studies were only able to reproduce auxin patterning, and an experimentally based mechanism for the simultaneous emergence of auxin and cytokinin patterning in the *Arabidopsis* root remained elusive. Here we show that the biological evidence discussed above is vital to explain the simultaneous patterning of auxin and cytokinin, while also allowing model predictions to match other experimental observations. Figure 1A summarises the mechanism in detail, and Figure 1B shows a simplified form, in which the red lines highlight the biological evidence discussed above. Specifically, this indicates that cytokinin promotes auxin biosynthesis, auxin promotes cytokinin biosynthesis, and ethylene signalling inhibits cytokinin degradation, so promoting cytokinin accumulation. As demonstrated below, combining such a mechanism with cell-to-cell communications simultaneously generates auxin and cytokinin patterning and also makes predictions that match independent experimental observations.

Journal Pre-proof

Relationship of auxin, cytokinin and ethylene in a homogenous cell following the mechanism

The mechanism shown in Figures 1A and 1B describes how auxin, cytokinin and ethylene mutually promote each other. For a cell without communications with other cells, Figure 2 shows that increasing any of auxin, cytokinin or ethylene biosynthesis rate always simultaneously enhances the concentration of all three hormones. For example, increasing or decreasing the key parameter for auxin biosynthesis by 1% from its value for wild type (Figure 2A) results in a similar increase or decrease of both auxin and cytokinin concentration by ca. 0.6%, while ethylene concentration increases or decreases by ca. 0.2%. Figure S1 shows an example of simultaneously enhancing the concentration of auxin, cytokinin and ethylene by increasing auxin biosynthesis rate in homogenous cells of the root.

The mechanism reproduces experimental observations of both auxin and cytokinin patterning in a realistic in silico root

The mechanism described in Figure 1 is a hormonal crosstalk network for auxin, ethylene and cytokinin extracted from a more complex auxin, ethylene and cytokinin network in Arabidopis root development (Liu et al., 2017). Investigating patterning requires the combination of a crosstalk network with a realistic digital root structure. A method to generate a 2-dimensional (2D) digital realistic root was previously developed and described in detail (Moore et al., 2017). The digital *in silico* root, as summarised in Figure 1 in Moore et al. (2017), is derived from experimental imaging and contains actual cell geometry and multicellular root organisation that allows the study of cell-cell communication (Band et al., 2014). In the *in silico* root, each cell contains two spatial identities: the cytosol, and the plasma membrane and cell wall, specific to each cell. For simplicity, adjacent plasma membrane and cell wall entities for the same cell are represented by a single identity containing both cell wall and plasma membrane properties. The *in silico* root also includes extracellular space but does not include any subcellular structures.

The regulation and placement of the auxin influx and efflux carriers (PIN1,2,3,4,7 and AUX1, LAX2,3 and ABCB) within the *in silico* root is based on experimental data as described previously (Moore et al., 2015, 2017). PIN1 and PIN2 carrier levels are regulated by the three hormones (Figure 1A). The rate that cytosolic PIN1 or PIN2 protein is placed at, and removed from, the plasma membrane was selected so that their polarity in the *in silico* root is similar to experimentally observed polarity (Moore et al., 2015, 2017). Other auxin carriers are prescribed based on experimental data because there is insufficient experimental data to establish how their levels and polarity are regulated by the three hormones (Moore et al., 2017). PIN3, PIN4 and PIN7 efflux carrier concentration levels and polar localisation have prescribed concentrations at selected cell faces based on experimental imaging described in the literature (Blilou et al., 2005). The non-polar auxin influx carriers AUX1, LAX2 and LAX3 also have prescribed localizations and levels based on experimental imaging (Band et al., 2014). The relative concentrations of PIN3, PIN4, PIN7, AUX1, LAX2 and LAX3 carriers are adjusted to generate wildtype auxin patterning. Since the ABCB family of auxin carriers can reversibly redirect auxin flux, the role of ABCB carriers in transporting auxin has been implicitly incorporated into the non-polar base level of PIN and AUX1/LAX activity, to simplify modelling analysis.

Where available, we have used parameter values from the literature (Moore et al., 2015, 2017). Since it is unknown if the biological knowledge accumulated in the literature is capable of simultaneously generating auxin and cytokinin patterning in the *Arabidopsis* root, we have adjusted the unknown parameters and examined the patterning of both auxin and cytokinin, to test the relationship between the known signalling interactions described above and the simultaneous patterning of auxin and cytokinin. Figures 3 and 4 show that the mechanism described in Figure 1, coupled with the realistic *in silico* root, can simultaneously generate auxin and cytokinin patterning that is in general agreement with experimental results. This indicates that the biological knowledge accumulated in the literature is sufficient to describe a mechanism to simultaneously generate auxin and cytokinin patterning in the *Arabidopsis* root.

Figures 3A and 3B show that the auxin concentration patterning generated by this mechanism is similar to auxin response patterning observed using DR5-GFP fluorescence. Figures 3A, 3C-3F display the auxin concentration patterning generated by this mechanism, showing patterning in the root tip (Figure 3A), and progressive enlargements in the elongation zone (Figures 3C, 3D) and QC region (Figures 3E, 3F). A pronounced auxin maximum occurs in the QC region (Figures 3A, 3E, 3F), with relatively high auxin levels in the columella and the root cap (Figures 3A, 3E). Auxin concentration declines, from the QC maximum, in the cell files above the initials and proximally up the vascular cylinder (Figures 3A, 3E). Interestingly, there is a clear increase in auxin concentration in the epidermis starting in the TZ and moving into the elongation zone (Figure 3A, 3C) and a similar but less obvious increase in the cortex (Figure 3A). Figures 3C and 3D show the existence of predicted auxin gradients within individual cells, with auxin declining at the proximal boundary of the epidermal cells in the elongation zone where the PIN efflux carriers remove auxin from the cell, and then increasing at the distal boundary of the neighbouring shootward cell due to the action of the auxin influx carriers. Auxin gradients may also emerge in extracellular space due to diffusion of auxin (Figures 3D, 3F).

Modelled auxin concentration patterning (Figures 3A, 3C to 3F) is in agreement with various experimental observations, including IAA distribution (Figure S2A; Figure 3 in Petersson et al., 2009), auxin response patterning *DR5::GFP* and *IAA2::GUS* (Figure S2B; S2C; Figures 3 and 4 in Grieneisen et al., 2007), and relative auxin levels based on the DII-VENUS inverse auxin response reporter (Figure S2D; Figure 2 in Brunoud et al., 2012). The different experimental observations give somewhat differing results for auxin patterning. The relative IAA distribution, based on cell sorting and mass spectrometry of various *Arabidopsis* lines, shows a distinct auxin maximum in the QC region, and higher auxin levels in the lateral root cap, cortex, endodermis and vascular cylinder compared to the columella and epidermis (Figure S2A; Figure 3 in Petersson et al., 2009). However, apart from the distinct differences between these regions the relative IAA distribution does not provide much additional information on auxin gradients. The *DR5::GFP* auxin response reporter (Figure S2B; Figure 3 in Grieneisen et al., 2007) identifies a high auxin response in the QC region and the proximal region of the columella, with the signal quickly declining in a shootward direction along the centre line of the vascular cylinder. There is no indication of relatively high auxin response in the lateral root cap or of an increase in the epidermis in the elongation zone (EZ). *In silico* results are in better agreement with the *IAA2::GUS* auxin reporter (Figure S2C; Figure 4 in Grieneisen et al., 2007), with a high auxin response in the QC region, columella and lateral root cap, and a proximally declining signal in the vascular cylinder. However, a noticeable difference between *in silico* results and experimental data using the *IAA2::GUS* reporter is that the reporter does not indicate a signal increase in the epidermis in the EZ. The auxin response image derived from the DII-VENUS auxin reporter (Figure S2D; Figure 2 in Brunoud et al., 2012) which gives an inverse auxin response signal, shows a maximum auxin response in the QC, high auxin response in the columella and lateral root cap, and a reduced response moving shootward along the vascular cylinder. In the epidermis, the response declines proximal to the initials and then starts to increase again at the beginning of the transition zone (TZ) , which is ca. longitudinal position 650 in Figure 3. *In silico* patterning is in good agreement with results generated by the DII-VENUS reporter (Figure S2D; Figure 2 in Brunoud et al., 2012). However, this epidermal patterning trend is not observable using *DR5::GFP* (Figure 3B; S2B). Following Brunoud et al. (2012), a possible explanation is that responses of these reporters can differ since *DR5* auxin response is also influenced by multiple signalling pathways.

Journal Pre-proof

Many features of *in silico* cytokinin concentration patterning (Figures 4A, 4C to 4F) are similar to those of *in silico* auxin patterning (Figures 3A, 3C to 3F). Cytokinin displays a maximum relative concentration in the QC region (but not to the same degree as auxin), with high concentrations in the columella and lateral root cap and with gradients similar to auxin in the vascular cylinder and epidermis.

Key features of the modelled cytokinin concentration patterning agree with experimental observations using ARR5-GFP fluorescence (Figure 4B) and other experimental observations as described below. The relative cytokinin concentration measured using cell sorting and mass spectrometry (Figure S3A; Figure 5 in Antoniadi et al., 2015) indicate high cytokinin concentrations in the QC region, columella and lateral root cap, medium concentrations in the vascular cylinder and in the epidermis and cortex in the TZ and EZ, and lower concentrations in the endodermis. The *in silico* concentration patterning (Figures 4A, 4C to 4F) is very similar to these experimental observations. Cytokinin response was also measured using the *ARR5::GUS* reporter (Figure S3B; Figure 3 in Werner et al., 2003) or using the *TCSn::GFP* reporter (Figure S3C; Figure 4 in Zurcher et al., 2013).

One marked difference between the experimental results for relative cytokinin concentration measurements (Figure S3A; Figure 5 in Antoniadi et al., 2015) and cytokinin response observations (Figure 4B; Figure S3B; Figure 3 in Werner et al., 2003; Figure S3C; Figure 4 in Zurcher et al., 2013) occurs in the QC region. While a high cytokinin concentration is measured in the QC by Antoniadi et al. (2015), a high cytokinin response is observed in the initials just proximal to the QC (Figure 4B; Figure S3B; Figure 3 in Werner et al., 2003; Figure S3C; Figure 4 in Zurcher et al., 2013). The modelled concentration patterning (Figure 4A) more closely matches the measured cytokinin concentration patterning in the QC (Figure S3A; Figure 5 in Antoniadi et al., 2015). A possible explanation for the difference between these experimental results is that cytokinin response is suppressed by the very high auxin concentration in the QC, via AHP6 signalling (Bishopp et al., 2011; Liu et al., 2017). On the other hand, Figures 4A and 4E also show that cytokinin concentration in a row of the cells below QC is noticeably lower. This is inconsistent with the measured cytokinin concentration patterning in those cells (Figure S3A; Figure 5 in Antoniadi et al., 2015). Thus, how AHP6 signalling regulates cytokinin response in those cells remains to be elucidated since modelled auxin concentration in those cells is relatively low (Figure 3).

Modelling predictions match a variety of experimental observations

The above results demonstrate that simultaneous patterning of both auxin and cytokinin in the *Arabidopsis* root (Figures 3 and 4) can emerge from a model based on a wide range of biological data. A further question is whether the mechanism can predict independent experimental observations. To predict different experimental outputs, we integrated the mechanism with the realistic digital root and parameters for reproducing simultaneous patterning of both auxin and cytokinin. This allows *in silico* predictions to be compared with a variety of experimental observations, generated both by our group and independently by other groups, as follows.

a) Auxin response trends in cell files above the initials

Relative auxin concentration trends in the epidermis, cortex, endodermis cells files above the initials were experimentally established using the R2D2 reporter (Figure S4A; Supplementary Figure 7 in Liao et al. 2015). Using the *in silico* wildtype, the auxin concentration was calculated at all grid points in the digital root. The average auxin concentration in each cell was then calculated by averaging all grid points within the cell. The computed auxin trends for the epidermis, cortex, and endodermis cells files above the initials (Figure 5A) closely match experimental results as shown by superimposing the in silico results onto the experimental graph (Figure S4B, C, D, E). Specifically, in all four cell layers, a significant decrease in auxin concentration is observed immediately in the cells above the initials, then the reduction in auxin concentration becomes much slower. In the epidermis, following the initial decrease, auxin concentration then increases slightly for the cells further above its initial. In the cortex and the pericycle the overall decrease in relative auxin concentration, in both experimental results and modelling results, is somewhat greater than observed in other cell layers. This demonstrates that the model is able to predict the pattern of auxin concentration for different tissues. However, when the four cell files are compared to each other, Figure S4F shows that for the cells near the initials, the level of the average auxin concentration does not follow a clear order. This is in contrast to experimental observations (Figure S4A), in which the average auxin concentration follows a clear order and sequentially decreases from epidermis, endodermis, cortex, to pericycle. For the cells further above the initials, the average auxin concentration follows the clear order that agrees with experimental observations. This indicates a limitation of the model to quantitatively predict the order of the average auxin concentration among some cells of the four cell files.

b) Auxin response minimum in the transition zone

Experimental results indicate that a minimum in the auxin response along the root axis (Figure S5A; Figure 3 in Di Mambro et al. 2017) occurs at the boundary of the proximal meristem and

Journal Pre-proof

Journal Pre-proof

distal transition zone, and that this minimum triggers a key developmental switch between cell division and cell differentiation (Di Mambro et al., 2017). Using the *in silico* wildtype, a longitudinal auxin concentration profile was calculated (Figure 5B) by progressively averaging auxin concentrations along the axis of the root (Figure 2A). The *in silico* results (Figure 5B) display an auxin concentration minimum in the distal TZ, similar to experimental observations (Figure S5A; Figure 3 in Di Mambro et al. 2017). Specifically, the longitudinal auxin concentration profile (Figure 5B) shows that auxin concentration decreases quickly from QC, approximately remains unchanged until above transition zone, then increases in the elongation zone. This demonstrates that, after both auxin and cytokinin patterning is fitted to experimental observations, an auxin concentration minimum intrinsically emerges in the distal TZ (Figure S5B).

c) Average auxin concentration trends in WT, *pls* mutant, *pls etr1* double mutant, and PLSox

Experimental data have demonstrated that up- or down-regulation of the *PLS* gene or the ethylene receptor protein ETR1 alters ethylene signalling responses (Casson et al. 2002; Chilley et al., 2006; Liu et al., 2010b). In *etr1* mutant, ethylene signalling response is up-regulated. Figure 5C shows that *in silico* predictions of the trend in average auxin concentration for the *pls* mutant, *pls etr1* double mutant, and the *PLS* overexpressing transgenic (*PLSox*), are in general agreement with experimental observations (Figure S6A; Figure 4C in Chilley et al. 2006). In the *pls* mutant, the experimentally measured auxin concentration is lower than in the wildtype; in the *pls etr1* double mutant auxin concentration is higher than the *pls* mutant, but still slightly lower than in the wildtype; and in PLS overexpressing seedlings, auxin concentration is higher than wildtype (Figure S6A; Figure 4C in Chilley et al. 2006). Modelled auxin concentration trends were superimposed over the experimental results (Figure S6B) and the modelled trends are in general agreement with experimental observations although, in the *pls etr1* double mutant, modelled auxin concentration is markedly lower than its experimental counterpart. PLS is a protein interacting with ethylene receptors (Casson et al. 2002; Chilley et al., 2006; Liu et al., 2010b; Mudge et al. 2023), and manipulating PLS activity affects ethylene signalling (Chilley et al., 2006; Liu et al., 2010b). Therefore, when both auxin and cytokinin patterning are fitted to experimental observations following the mechanism (Figure 1), the effects of genetic manipulation of ethylene signalling on average auxin concentration in the root can also be predicted.

d) Patterning the rate of auxin biosynthesis

The rate of auxin biosynthesis also demonstrates patterning in the root tip (Figure S7; Figure 5 in Petersson et al. 2009). Using the *in silico* wildtype simulation, the computed patterning of the rate of auxin biosynthesis shows high levels of biosynthesis in the columella and the QC region, lower levels in the TZ, and an increase in biosynthesis rates in the epidermis, cortex and central vascular cylinder in the EZ. There is a close match between experimental (Figure S7; Figure 5 in Petersson et al. 2009) and predicted auxin biosynthesis rate patterning (Figure 5D). Thus, the proposed mechanism is not only able to predict important features of auxin concentration patterning, but also to predict patterning of the rate of auxin biosynthesis. Therefore, auxin patterning, transport and metabolism are elucidated as an integrated system in this work.

e) The average concentration trend of PIN1 and PIN2 proteins in WT, PLSox transgenic, *pls* and *etr1* mutants, and *pls etr1* double mutant.

Immunolocalization experiments (Figure S8; Figure 1B in Liu et al. 2013) showed that both PIN1 and PIN2 protein levels increase in the *pls* mutant and decrease in PLSox compared to wildtype; in the ethylene-insensitive *etr1* mutant PIN1 and PIN2 levels are lower than in wildtype; and the *pls etr1* double mutant exhibits reduced PIN1 and PIN2 levels compared to *pls* and is marginally lower than wildtype. The *in silico* trends for these mutants (Figure 6A) are similar to experimental observations, demonstrating that the proposed mechanism is able to predict changes in PIN1 and PIN2 levels, and therefore predict how genetic manipulations can alter the average auxin transporter concentration in the root.

f) Predicted changes in PIN1 and PIN2 concentrations in *pin3*, *pin4*, *pin7* mutants

So far, we have demonstrated that the *in silico* wildtype simulation is able to predict many features of auxin patterning and trends in auxin, and PIN1 and PIN2 levels in various mutants. A further question is whether PIN1 and PIN2 patterning changes can also be predicted.

Production and degradation of both PIN1 and PIN2 in a cell is assumed to follow the same mechanism based on experimental observations as analysed previously (Moore et al. 2015; 2017; Liu et al. 2013). However, PIN1 and PIN2 are distinguished by their polarity and location settings in different parts of the root tip.

Figure 6B shows *in silico* predictions for the percentage change in PIN1 or PIN2 concentrations relative to WT for the *pin3, pin4* and *pin7* single mutants and the *pin3pin4pin7* triple mutant. Figure 6C is an enlargement of the proximal vasculature for the *pin4* single mutant image in Figure 6B. Modelled change in PIN1 patterning for the *pin3*, *pin4* and *pin7* single mutants (Figures 6B and 6C) is similar to experimental observations (Figure S9A;

Figure 6 in Omelyanchuk et al. 2016). In particular, the region of PIN1 expression extends shootward up the vasculature in these mutants (Figure S9A; Figure 6 in Omelyanchuk et al. 2016).

The modelled PIN1 concentration changes in the *pin3* mutant versus wildtype (Figure6B) shows a significant increase in the proximal vasculature and in the columella. This is consistent with experimentally observed PIN1 expression in the same mutant (Figure S9A; Figure 6 in Omelyanchuk et al. 2016).

Moreover, the modelled PIN1 concentrations in the *pin4* mutant show slight increases at the plasma membrane in the proximal vasculature (Figure 6B). This is consistent with experimental *pin4* mutant observations (Figure S9A; Figure 6 in Omelyanchuk et al. 2016).

In addition, the modelled PIN1 patterning change in the *pin7* mutant (Figure 6B) is similar to experimental observations (Figure S9A; Figure 6 in Omelyanchuk et al. 2016), in which an increase in *PIN1* concentration can be seen in the proximal vasculature of the *pin7* mutant.

Thus, the integrative mechanism for the simultaneous auxin and cytokinin patterning is able to make correct predictions on the change of PIN1 patterning in *pin3*, *pin4* and *pin7* mutant.

In addition, experimental observations show changes in PIN2 patterning in the *pin3pin4pin7* triple mutant. A clear increase in PIN2 level in the vasculature emerges (Figure S9B; Figure 1 in Blilou et al. 2005). Modelled change in PIN2 patterning for the *pin3pin4pin7* triple mutant predicts a significant increase in PIN2 concentrations in the vasculature (Figure 6B), which is consistent with experimental observation (Figure S9B; Figure 1 in Blilou et al. 2005).

These results indicate that the integrative mechanism proposed in this research predicts the main features of patterning change in PIN1 and PIN2 concentration in *pin3*, *pin4*, *pin7* mutants and as such elucidates how PIN1 and PIN2 patterning changes in single and triple *pin* mutants.

g) Cytokinin patterning and concentration change in *pls* mutant.

Figures 5 and 6 demonstrate that the mechanism described in Figure 1 is able to predict patterning and/or trends in auxin concentration, auxin biosynthesis rate, and PIN1,2. The mechanism can also predict patterning and concentration change for cytokinin in pls mutant.

First, auxin, cytokinin, and ethylene all regulate gene expression (Binder 2020; Kieber and Schaller 2018; Weijers and Wagner 2016). *PLS* gene expression is regulated by both auxin and ethylene (Chilley et al., 2006; Liu et al. 2010). Modelled patterning of *PLS* expression

Journal Pre-proof

predicts measured proPLS::PLS:GFP fluorescence (Figure 7A). Modelled PLS levels are high in the columella, lateral root cap and QC region, which is consistent with experimental observations (Figure 7A). This demonstrates that the mechanism proposed in this research is also able to predict gene expression patterning.

PLS protein has a role in regulating ethylene signalling (Chilley et al., 2006; Liu et al. 2010) that in turn regulates auxin and cytokinin concentration and signalling (Figure 1). Thus, an important question is how PLS patterning regulates concentration and patterning of other components in Figure 1.

Figure 7B predicts that, in the *pls* mutant, modelled cytokinin concentration has a 1.48 -fold increase relative to wildtype. This compares favourably to experimental results (Table 1 in Liu et al., 2010) that show a 1.42 median fold increase. In addition, modelling reveals that cytokinin concentration in *pls* shows a significant increase in the columella, lateral root cap and QC region (Figure 7C), which is similar to experimental observations using TCSn:GFP fluorescence (Figure 7D). Thus, effects of *pls* mutant on the concentration and patterning of cytokinin are correctly predicted by the mechanism proposed in this research (Figure 1).

In addition, Figure S10 predicts that ethylene concentration in *pls* mutant is the same as that in wildtype. This is consistent with experimental observations (Chilley et al., 2006).

Modelling reveals the role of regulatory relationships in auxin and cytokinin concentration and patterning

So far, we have demonstrated that the model based on the mechanism, Figure 1, is able to not only generate simultaneous patterning of both auxin and cytokinin, but also predict a variety of experimental observations. Here we further show that the model is able to develop insights into the role of regulation in auxin and cytokinin patterning.

a) Auxin influx and efflux transporters are the key driver for auxin patterning

Figure S11 shows that auxin patterning still emerges when auxin biosynthesis is not regulated by cytokinin or ethylene with all auxin transporters being fixed as those in the wildtype. This indicates auxin influx and efflux transporters are the key players for generating auxin patterning. Moreover, both cytokinin and ethylene patterning still emerges. However, Figure S11 also reveals that the percentage change in the concentration of auxin, cytokinin and ethylene is different in different cells, and therefore the regulation of auxin biosynthesis plays a fine-tuning role in patterning. In the absence of auxin biosynthesis regulation, Figures S12, S13 and S14 show that predictions about the trends in different mutants (Figure S12C, S12D, S13A, S14B) are affected. In particular, the patterning of auxin biosynthesis rate cannot be predicted anymore (Figure S12D). In addition, Figure S11 shows that the concentration of auxin, cytokinin and ethylene in the epidermis is higher than that in the cortex. This is consistent with the mutual positive regulation of auxin, cytokinin and ethylene (Figure 1, 2, S1). This high concentration in epidermis still exists when the regulation of auxin biosynthesis by ethylene and cytokinin is removed, but it is generally less obvious since the percentage reduction relative to wildtype is relatively large (Figure S11). High concentration in epidermis was also previously modelled (Band et al. 2014) in the absence of regulation in auxin biosynthesis. Therefore, regulation of auxin biosynthesis plays a fine-tuning role in the high auxin concentration in the epidermis. Figure 2, 3, S11 also show that the intracellular gradient of auxin, cytokinin and ethylene in epidermis is large. To the best of our knowledge, no experimental observations about this gradient have been observed.

b) Regulation of cytokinin degradation by ethylene signalling is important for predicting auxin and cytokinin concentration trend in mutants

Figure S15, S16, S17 show that, in the absence of the regulation of cytokinin degradation by ethylene signalling, auxin concentration trend in mutants and patterning in auxin biosynthesis rate are incorrectly predicted (Figure 15C; 15D). Moreover, Figure S17B predicts a lower average cytokinin concentration in *pls* mutant than that in wildtype, which is opposite to experimental observations (Figure 5).

c) Regulation of cytokinin biosynthesis by auxin signalling is important for predicting auxin concentration trend in mutants and patterning of auxin biosynthesis rate

Figures S18, S19, S20 show that, in the absence of the regulation of cytokinin biosynthesis by auxin signalling, auxin concentration trend in mutants and patterning in auxin biosynthesis rate are incorrectly predicted (Figure 18C; 18D). Moreover, Figure 20C shows that cytokinin patterning does not emerge anymore.

d) Role of changes in PIN1 and PIN2 concentration and patterning in various mutants

Figures S21, S22, S23 and S24 show that changes in PIN1 and PIN2 concentration and patterning in *pin3*, *pin4*, *pin7* or *pin3,4,7* mutants play a fine-tuning role in the concentration and patterning of auxin, cytokinin and ethylene. Interestingly, they differentially affect different cells. For example, in *pin3,4,7* triple mutant, if PIN1 and PIN2 are fixed at wildtype levels, auxin concentration in some stele and columella cells increases with a larger percentage.

e) Role of various mutants related to ethylene signalling

In addition to the analysis of the role of regulatory relationships in auxin and cytokinin concentration and patterning, modelling can also predict the role of various mutants for future experimental validations. For example, Figures S25, S26, S27 and S28 reveal that various mutants related to ethylene signalling can simultaneously change the concentration and patterning of auxin, cytokinin and ethylene.

DISCUSSION

By interrogating and integrating biological knowledge, this research has revealed a mechanism for the simultaneous patterning of auxin and cytokinin in the *Arabidopsis* root. Based on modelling of the mechanism and experimental investigations, this research reveals that simultaneous auxin and cytokinin concentration patterning emerges from multi–level regulation of auxin, cytokinin and ethylene in the root, as summarised in Figure S29.

The mechanism not only simultaneously generates auxin and cytokinin patterning that agrees with experimental observations in the *Arabidopsis* root (Figures 2, 3), but also makes a wide range of predictions that are validated by experimental measurements generated by our group and by independent experimental observations generated by other groups (Figures 5,6,7). Therefore, we consider that the mechanism is plausible, based on current knowledge.

This mechanism suggests some important aspects about simultaneous patterning of auxin and cytokinin, with a novel key role played by ethylene. The following regulatory relationships are important for simultaneously generating auxin and cytokinin patterning. First, cytokinin promotes auxin biosynthesis (Jones et al., 2010), auxin upregulates cytokinin biosynthesis through SHY2 and IPT5 (Dello Ioio et al., 2008), and auxin promotes cytokinin biosynthesis through TM05 and LOG4 (De Rybel et al., 2014). This compares to previously proposed regulatory relationships (Moore et al., 2015), where auxin inhibited cytokinin biosynthesis and cytokinin inhibited auxin biosynthesis (based on Nordstrom et al., 2004) which, while generating auxin patterning similar to experimental observation, could not generate representative cytokinin patterning. Second, a novel ethylene regulatory link is also important for the simultaneous patterning of auxin and cytokinin, and for the simulation to predict a range of experimental results. This new regulatory link is based on experimental evidence discussed in this manuscript and in Liu et al. (2017). Briefly, an ETR1-dependent phospho-relay promotes ARR2 phosphorylation and activity, ARR2 promotes *CKX* expression and activity, and cytokinin degradation occurs through the action of a set of CKX (Werner et al., 2003, 2006). These and other experimental observations (Kim et al., 2012; Werner et al., 2003; Werner et al., 2006; To et al., 2007, Hass et al., 2004) establish the regulation of cytokinin concentration by ethylene signalling through components of the cytokinin pathway. Inclusion of these regulatory links generates simultaneous patterning of both auxin and cytokinin similar to experimental observations and in addition enables the mechanism to predict a variety of experimental observations (Figures 3 to 7).

This research therefore demonstrates that, although the regulation of auxin, cytokinin and ethylene concentration in *Arabidopsis* root is very complex (Liu et al., 2017), and the experimental data available in the literature are diverse, the integration of the available experimental data is able to derive a plausible mechanism to both study the patterning of auxin and cytokinin as an integrative system and also predict various experimental observations. As a result, this work proposes a mechanism which enables the rational study of the complex and important simultaneous regulation of auxin and cytokinin patterning.

Since auxin and cytokinin responses are induced by their concentrations, it is reasonable to consider that auxin and cytokinin response patterning is closely related to auxin and cytokinin concentration patterning. In principle, the mechanism proposed in this work can be extended to analyse auxin and cytokinin responses by establishing links between concentration and response. However, the relationship between concentration and response is generally nonlinear. For example, it was shown that modelling the response of DII-VENUS reporter to auxin requires a model to describe the nonlinear relationship between DII-VENUS and auxin concentration (Band et al. 2012). Moreover, given the complexity of the pathways and multiple links between pathways (Liu et al., 2017), all hormone responses will, to varying degrees, be regulated by multiple hormone activity. Two good examples of this are the regulation of the cytokinin response regulator ARR5 by both ethylene and cytokinin, and the regulation of cytokinin response by both cytokinin and auxin through AHP6 (Liu et al., 2017). Thus, response modelling may require analysis of how interactions between multiple hormones determine response levels. For example, it was shown that elucidating cytokinin response also needs to consider response regulation by auxin (De Rybel et al., 2014). A gene regulatory network involving both auxin and cytokinin establishes and maintains vascular patterning (Muraro et al. 2014). Moreover, the link from transverse auxin fluxes to lateral root initiation is regulated by both auxin and cytokinin (el-Showk et al., 2015). Importantly, all of these studies demonstrate that relationships between auxin and cytokinin concentration and response are nonlinear (Mellor et al., 2017). Thus, establishing the link between hormone concentration and

Journal Pre-proof

response needs to carefully establish the various concentration-to-response relationships based on relevant experimental data.

Cytokinin movement in the root can be passive via diffusion but can also be regulated by cytokinin transporters. This work considers that cytokinin movement is via diffusion due to lack of knowledge about distribution of cytokinin transporters in the root and the kinetics of such transporters (Kang et al., 2017). Once the kinetics of cytokinin transporters have been established, interesting future research can include the study of how the cytokinin transporters and cytokinin diffusion work together to transport cytokinin and influence patterning and development.

Extracting a mechanism for simultaneously patterning of auxin and cytokinin necessitates the simplification of complex interactions between multiple hormones. The mechanism (Figure 1) is a simplified version of the more complex network of interactions between auxin, cytokinin and ethylene summarised in Liu et al. (2017). In the mechanism, auxin, cytokinin and ethylene are assumed to regulate PIN1 and PIN2 in the same way. This assumption was based on the analysis of a variety of experimental data (Liu et al. 2013; Moore et al., 2015, 2017). Although the main features of patterning changes in PIN1 and PIN2 concentration in *pin3*, *pin4*, *pin7* mutants (Figure 6) can be predicted using the proposed mechanism, a feature in which enhanced PIN1 protein was detected in lateral-basal membranes of the endodermis in *pin3*, *pin4*, *pin7* triple mutant (Blilou et al. 2005) cannot be predicted using the mechanism. This could imply that, while the regulation of both PIN1 and PIN2 by auxin, cytokinin and ethylene can be largely described by the same relationships as described by Figure 1, some subtle differences in the regulatory relationships may exist. Thus, the regulation of PIN1 and PIN2 may need to be further refined experimentally and computationally in the future. Therefore, formulating a mechanism such as Figure 1 in this work, while making a variety of predictions, can also identify knowledge gaps by highlighting differences between predictions and experimental observations.

With various experimental data being accumulated and new data becoming available, it is evident that elucidating the role of the complex regulatory relationships of multiple hormones in plant development is becoming a major challenge (Schaller et al., 2015; Liu et al., 2017). This work demonstrates that integrating such data can unravel a mechanism for simultaneous patterning of auxin and cytokinin in the *Arabidopsis* root. Various predictions indicate that a variety of experimental observations can also be elucidated by the same mechanism. By integrating additional hormones in the future, the regulation of multiple hormone concentration and response patterning in the *Arabidopsis* root can be quantitatively and rationally explored.

METHODS

Plant materials

Arabidopsis seed were obtained from lab stocks or from the Nottingham *Arabidopsis* Stock Centre (NASC). All mutant and reporter lines are in Col-0 background except *pls* (C24). Seedlings were grown on 10 cm square plates of 1/2 Murashige and Skoog agar media sealed with micropore tape as described (Chilley *et al.* 2006). Seedlings were grown in SANYO growth cabinets (22C°, 18hr photoperiod).

Microscopy and image analysis

Prior to confocal imaging, TCSn:GFP, *pls-3/*TCSn:GFP, R2D2, proPIN3:PIN3:GFP and proPIN7:PIN7:GFP seedlings were fixed using the ClearSee method previously described by Kurihara *et al.* (2015). The ClearSee protocol enables rapid fixing and clearing of plant tissues whilst retaining the activity of fluorescent proteins and is compatible with various fluorescent dyes (Ursache *et al.* 2018)

To prepare 4% paraformaldehyde (PFA) solution for the fixing procedure, 4 g of PFA powder was added to 1L of 1x phosphate-buffered saline (PBS) solution on a magnetic stirrer and heated to around 60 °C. To ensure the PFA powder is dissolved, the pH was raised using 1M KOH until the solution is clear. The pH was then adjusted to 6.9 with 1M HCL solution. The solution was cooled and filtered before use. The PFA solution was used fresh or kept a 4C° and used within a week.

Seedlings were transferred with forceps to the 4% PFA solution where they were fixed under vacuum for 30 minutes. Following fixation, seedlings were washed in 1X PBS solution twice before the addition of ClearSee solution, where they were again placed under vacuum for 30 minutes.

ClearSee solution is prepared via mixing together xylitol (10% w/v), sodium deoxycholate (15% w/v) and urea (25% w/v) and H_2O in a solution for 30 minutes. Fixed seedlings were left in ClearSee solution at room temperature for at least a week with the ClearSee replaced every few days. Following clearing, seedlings were stained and imaged.

Journal Pre-proof

Seedlings were examined using a Zeiss LCSM 800 or LCSM 880 (https://www.zeiss.com/-microscopy/int/home.html). Roots were imaged using either a x10 or x20 air objective lens. Z-stacks were taken of each seedling to gain the maximum information possible. Settings such as gain, line, Z-step, averaging etc. were altered between each fluorescent reporter to optimise image quality and consistency.

To visualise cell structure and organisation under LCSM, cleared seedlings were submerged in 0.1% Calcoflour White in ClearSee solution for 30 minutes. Following staining, Calcolfuor White solution was replaced by ClearSee and seedlings were washed for another 30 minutes. For LCSM, fixed seedlings were mounted on sides in ClearSee solution under a coverslip.

Digital root construction and spatiotemporal modelling

The details for construction of a digital root, numerical methods, averaging hormone concentration for a cell, and averaging hormone concentration in the digital root were previously reported (Moore et al. 2015; 2017; Liu et al. 2017) and remain the same for this research. In particular, digital root structure with actual cell geometries, polar localisation of efflux carriers and nonpolar localisation of influx carriers were described in detail (Moore et al. 2017; Liu et al. 2017). The images of PIN1,2,3,4,7 and AUX1 and LAX2,3 were shown in Moore et al. 2017. The parameter values for modelling equations in this research are included in Table S1, S2 and S3.

Comparison of modelling and experimental results

Comparison of modelling and experimental results in this research focuses on longitudinal trends along the root and does not attempt to make quantitative comparison at cell or pixel level for the following reasons. i) Although the modelled digital root was constructed based on the typical anatomy of an *Arabidopsis* root and although it includes important root features such as type, geometry, size and wall of each cell, and extracellular matrix (Moore et al. 2015; Liu et al. 2017), the cell size, geometry or wall location in the digital root is not exactly the same as its counterpart in experimental images of any individual root. Therefore, it is impossible to make direct quantitative comparison with experimental images at a cellular or pixel level. ii) Experimental images in our experiments and those in the literature generally show the trends and patterning of measured components and generally do not quantify actual concentrations of any components. Thus, direct concentration comparison is not as important as trend and pattern comparison. iii) Biologically, patterning generally refers to trend or gradient change, and is considered to play a crucial role in root development. Thus, comparisons between modelled and experimental results in this research concentrates on the similarity or differences in trends and patterning.

SUPPLEMENTAL INFORMATION

Supplemental information is available at *Plant Communications Online.*

FUNDING

J.L. and K.L. gratefully acknowledge Research Councils UK and the Biotechnology & Biological Sciences Research Council (BB/E006531/1) for funding in support of this study; G.J. acknowledges receipt of a BBSRC DTP studentship (BB/M011186/1). C.C. gratefully acknowledges Advanced Foreign Experts Project (G2023157014L) and the Cultivating Fund Project of Hubei Hongshan Laboratory (2022hspy002).

Journal Pre-proof

AUTHOR CONTRIBUTIONS

J.L. and K.L. initiated the project; S.M., J.L. and K.L. designed modelling and experimental study and drafted the manuscript; J.L., K.L. J.F.T and C.C. supervised the study; S.M., J.L. and G.J. carried out modelling and experimental work; all authors edited the final draft of the manuscript.

ACKNOWLEDGEMENTS

The authors declare no conflicts of interest.

Journal Pre-proof

REFERENCES

Antoniadi, I., Plackova, L., Simonovik, B., Dolezal, K., Turnbull, C., Ljung, K., Novak, O. (2015). Cell-type-specific cytokinin distribution within the *Arabidopsis* primary root apex. Plant Cell **27**: 1955-1967.

Bagdassarian, K.S., Etchells,J.P., Savage N.S. (2023). A mathematical model integrates diverging PXY and MP interactions in cambium development. in silico Plants **5**: 1–15

Band, L.R., Wells, D.M., Larrieu, A., Sun, J., Middleton, A.M., French, A.P., Brunoud, G., Sato, E.M., Wilson, M.H., Péret, B., Oliva, M., Swarup, R., Sairanen, I., Parry, G., Ljung, K., Beeckman, T., Garibaldi, J.M., Estelle, M., Owen, M.R., Vissenberg, K., Hodgman, T.C., Pridmore, T.P., King, J.R., Vernoux, T., Bennett, M.J. (2012). Root gravitropism is regulated by a transient lateral auxin gradient controlled by a tipping-point mechanism. Proc. Natl. Acad. Ssci. USA **109**: 4668–4673.

Band, L.R., Wells, D.M., Fozard, J.A., Ghetiu, T., French, A.P., Pound, M.P., Wilson, M.H., Yu, L., Li, W., Hijazi, H.I., Oh, J., Pearce, S.P., Perez-Amador, M.A., Yun, J., Kramer, E., Alonso, J.M., Godin, C., Vernoux, T., Hodgman, T.C., Pridmore, T.P., Swarup, R., King, J.R., Bennett, M.J. (2014). Systems analysis of auxin transport in the *Arabidopsis* root apex. Plant Cell **26**: 862–875.

Binder, B.M. (2020). Ethylene signaling in plants. J. Biol. Chem. **295**: 7710–7725.

Bishopp, A., Help, H., El-Showk, S., Weijers, D., Scheres, B., Benkova, E., Friml, J., Mahonen, A.P., Helariutta, Y. (2011). A mutually inhibitory interaction between auxin and cytokinin specifies vascular pattern in roots. Curr. Biol. **21**: 917–926.

Blilou, I., Xu, J., Wildwater, M., Willemsen, V., Paponov, I., Friml, J., Heidstra, R., Aida, M., Palme,. K, Scheres, B. (2005). The PIN auxin efflux facilitator network controls growth and patterning in *Arabidopsis* roots. Nature **433**: 39-44.

Brunoud, G., Wells, D.M., Oliva, M., Larrieu, A., Mirabe,t V., Burrow, A.H., Beeckman, T., Kepinski, S., Traas, J., Bennett, M.J., Vernoux, T. (2012). A novel sensor to map auxin response and distribution at high spatio-temporal resolution. Nature **482**: 103–106.

Cancel, J.D., Larsen, P.B. (2002). Loss-of-function mutations in the ethylene receptor ETR1 causes enhanced sensitivity and exaggerated response to ethylene in *Arabidopsis*. Plant Physiol. **129**: 1557–1567.

Casanova-Sáez, R., Mateo-Bonmatí. E., Ljung, K. (2021). Cold Spring Harb. Perspect. Biol. **13**: a039867

Casson, S.A., Chilley, P.M., Topping, J.F., Evans, I.M., Souter, M.A., Lindsey, K. (2002). The *POLARIS* gene of *Arabidopsis* encodes a predicted peptide required for correct root growth and leaf vascular patterning. Plant Cell **14**: 1705–1721.

Chandler, J.W., Werr, W. (2015). Cytokinin–auxin crosstalk in cell type specification. Trends Plant Sci. **20**: 291–300.

Journal Pre-proof

Journal Pre-proof

Chatfield, J.M., Armstrong, D.J. (1986). Regulation of cytokinin oxidase activity in callus tissues of *Phaseolus vulgaris* L. cv Great Northern. Plant Physiol. **80**: 493-499.

Chilley, P.M., Casson, S.A., Tarkowski, P., Hawkins, N., Wang, K.L., Hussey, P.J., Beale, M., Ecker, J.R., Sandberg, G.K., Lindsey, K. (200)6. The POLARIS peptide of *Arabidopsis* regulates auxin transport and root growth via effects on ethylene signaling. Plant Cell **18**: 3058–3072.

Colin, L., Martin-Arevalillo, R., Bovio, S., Bauer, A., Vernoux, T., Caillaud, M.C., Landrein, B., Jaillais, Y. (2022). Plant Cell **34**: 247–272.

De Rybel, B., Adibi, M., Breda, A.S., Wendrich, J.R., Smit, M.E., Novák, O., Yamaguchi, N., Yoshida, S., Van Isterdael, G., Palovaara, J., Nijsse, B., Boekschoten, M.V., Hooiveld, G., Beeckman, T., Wagner, D., Ljung, K., Fleck, C., Weijers, D. (2014). Integration of growth and patterning during vascular tissue formation in *Arabidopsis*. Science **345**: 1255215-1–1255215-8.

Dello Ioio, R., Nakamura, K., Moubayidin, L., Perilli, S., Taniguchi, M., Morita, M.T., Aoyama, T., Costantino, P., Sabatini, S. (2008). A genetic framework for the control of cell division and differentiation in the root meristem. Science **322**: 1380–1384.

Di Mambro, R., De Ruvo, M., Pacifici, E., Salvi, E., Sozzani, R., Benfey, P.N., Busch, W., Novak, O., Ljung, K., Di Paola, L., Marée, A.F.M., Costantino, P., Grieneisen, V.A., Sabatini, S. (2017). Auxin minimum triggers the developmental switch from cell division to cell differentiation in the *Arabidopsis* root. Proc. Natl. Acad. Sci. USA **114**: E7641–E7649

El-Showk, S., Ruonala, R., Helariutta, Y. (2013). Crossing paths: cytokinin signaling and crosstalk. Development **140**: 1373-1383

El-Showk, S., Help-Rinta-Rahko, H., Blomster, T., Siligato, R., Marée, A.F.M., Mähönen, A.P., Grieneisen, V.A. (2015). Parsimonious model of vascular patterning links transverse hormone fluxes to lateral root initiation: auxin leads the way, while cytokinin levels out. PLoS Comput. Biol. **11**: 1–40.

Friml, J. (2021). Fourteen stations of auxin. Cold Spring Harb. Perspect. Biol **14**: a039859

Garcia-Gomez, M.L., Azpeitia, E.,Alvarez-Buylla, E.R. (2017) A dynamic genetic-hormonal regulatory network model explains multiple cellular behaviors of the root apical meristem of *Arabidopsis* thaliana. PLoS Comput Biol 13(4): e1005488.

García-Gómez, M.L., Ornelas-Ayala, D., Garay-Arroyo, A., GarcíaPonce, B., Sánchez. M.P., Álvarez-Buylla, E.R. (2020) A system-level mechanistic explanation for asymmetric stem cell fates: *Arabidopsis* thaliana root niche as a study system. Scientific Reports **10**: 3525

Garay-Arroyo, A., De La Paz, S.M., Garcıa-Ponce, B., Azpeitia, E., Alvarez-Buylla, E.R. (2012). Hormone symphony during root growth and development. Developmental Dynamics **241**: 1867–1885.

Grieneisen, V.A., Xu, J., Maree, A.F.M., Hogeweg, P., Scheres, B. (2007). Auxin transport is sufficient to generate a maximum and gradient guiding root growth. Nature **449**: 1008–1013.

Hass, C., Lohrmann, J., Albrecht, V., Sweere, U., Hummel, F., Yoo, S., Hwang, I., Zhu, T., Schafer, E., Kudla, J., Harter, K.T. (2004). The response regulator 2 mediates ethylene signaling and hormone signal integration in *Arabidopsis*. EMBO J. **23**: 3290–3302

Hwang, I., Sheen, J. (2001). Two-component circuitry in *Arabidopsis* cytokinin signal transduction. Nature **413**: 383-389

Isoda, R., Yoshinari, A., Ishikawa, Y., Sadoine, M., Simon, R., Frommer, W.B., Nakamura, M. (2021). Sensors for the quantification, localization and analysis of the dynamics of plant hormones. Plant J. **105**: 542–557.

Jones, B., Gunneras, S.A., Petersson, S.V., Tarkowski, P., Graham, N., May, S., Dolezal, K., Sandberg, G., Ljung, K. (2010). Cytokinin regulation of auxin synthesis in *Arabidopsis* involves a homeostatic feedback loop regulated via auxin and cytokinin signal transduction. Plant Cell **22**: 2956–2969.

Jones, B., Ljung, K. (2011). Auxin and cytokinin regulate each other's levels via a metabolic feedback loop. Plant Sign. Behav. **6**: 901–904.

Kang, J., Lee, Y., Sakakibara, H., Martinoia, E. (2017). Cytokinin Ttransporters: GO and STOP in signaling. Trends Plant Sci. **22**: 455–461.

Kieber, J., Schaller, G.E. (2018). Cytokinin signaling in plant development. Development **145**: dev149344.

Kim, K., Ryu, H., Cho, Y., Scacchi, E., Sabatini, S., Hwang, I. (2012). Cytokinin-facilitated proteolysis of *ARABIDOPSIS* RESPONSE REGULATOR attenuates signaling output in two component circuitry. Plant J. **69**: 934–945.

Kurihara, D., Yoko, M., Yoshikatsu, S., Tetsuya, H. (2015). Clearsee: A rapid optical clearing reagent for whole-plant fluorescence imaging. Development **142**: 4168-4179.

Kushwah, S., Jones, A.M., Laxmi, A. (2011). Cytokinin interplay with ethylene, auxin, and glucose signaling controls *Arabidopsis* seedling root directional growth. Plant Physiol. **156**: 1851–1866.

Liao, C.-Y., Smet, W., Brunoud, G., Yoshida, S., Vernoux, T., Weijers, D. (2015). Reporters for sensitive and quantitative measurement of auxin response. Nature Methods **12**: 207–210.

Liu, J.L., Mehdi, S., Topping, J., Tarkowski, P., Lindsey, K. (2010). Modelling and experimental analysis of hormonal crosstalk in *Arabidopsis*. Molec. Systems Biol. **6**: 373.

Liu, J.L., Mehdi, S., Topping, J., Friml, J., Lindsey, K. (2013). Interaction of PLS and PIN and hormonal crosstalk in *Arabidopsis* root development. Front. Plant Sci. **4**: 75

Journal Pre-proof

Liu, J., Moore, S., Chen, C., Lindsey, K. (2017). Crosstalk complexities between auxin, cytokinin, and ethylene in *Arabidopsis* root development: From experiments to systems modeling, and back again. Molec. Plant. **4**: 1480-1496.

Ljung,, K. (2013). Auxin metabolism and homeostasis during plant development. Development **140**: 943–950.

Ludwig-Müller, J. (2011). Auxin conjugates: their role for plant development and in the evolution of land plants. J. Exp. Bot. **62**: 1757–1773.

Muraro, D., Byrne, H., King, J., Voß, U., Kieber, J., and Bennett, M. (2011). The influence of cytokinin–auxin cross-regulation on cell-fate determination in *Arabidopsis* thaliana root development. J. Theor. Biol. **283**:152–167.

Muraro, D., Byrne, H., King, J., and Bennett, M. (2013). The role of auxin and cytokinin signalling in specifying the root architecture of *Arabidopsis* thaliana. J. Theor. Biol. **317**:71–86.

Muraro, D., Mellor, N., Pound, M.P., Help, H., Lucas, M., Chopard, J., Byrne, H.M., Godin, C., Hodgman, T.C., King, J.R., et al. (2014). Integration of hormonal signaling networks and mobile microRNAs is required for vascular patterning in *Arabidopsis* roots. Proc. Natl. Acad. Sci. USA **111**:857–862.

Muraro, D., Larrieu, A., Lucas, M., Chopard, J., Byrne, H., Godin, C., and King, J. (2016). A multi-scale model of the interplay between cell signalling and hormone transport in specifying the root meristem of *Arabidopsis* thaliana. J. Theor. Biol. **404**:182–205.

Mellor, N., Adibi, M., El-Showk, S., De Rybel, B., King, J., Mahonen, A.P., Weijers, D., Bishopp, A. (2017). Theoretical approaches to understanding root vascular patterning: a consensus between recent models. J. Exp. Bot. **68**: 5–16.

Mellor, N., Vaughan-Hirsch, J., Kumpers, B.M.C., Help-Rinta-Rahko, H., Miyashima, S., Mahonen, A.P., Campilho, A., King, J.R., and Bishopp, A. (2019). A core mechanism for specifying root vascular patterning can replicate the anatomical variation seen in diverse plant species. Development **146**, dev172411.

Moore, S., Zhang, X., Mudge, A., Rowe, J.H., Topping, J.F., Liu, J., Lindsey, K. (2015). Spatiotemporal modelling of hormonal crosstalk explains the level and patterning of hormones and gene expression in *Arabidopsis* thaliana wildtype and mutant roots. New Phytol. **207**: 1110–1122.

Moore, S., Liu, J., Zhang, X., Lindsey, K. (2017). A recovery principle provides insight into auxin pattern control in the *Arabidopsis* root. Sci. Rep. **7**: 430004.

Mudge, A., Mehdi, S., Michaels, W., Orosa-Puente, B., Shen, W., Sadanandom, A., Hetherington, F., Hoppen, C., Unzen, B., Groth, G., Topping, J.F., Robinson, N.J., Lindsey, K. (2023). A peptide that regulates the metalation and function of the *Arabidopsis* ethylene receptor. BioRxiv https://doi.org/10.1101/2023.06.15.545071.

Muraro, D., Mellor, N., Pound, M.P., Help, H., Lucas, M., Chopard, J., Byrne, H.M., Godin, C., Hodgman, T.C., King, J.R., Pridmore, T.P., Helariutta, Y., Bennett, M.J., Bishopp, A. (2014). Integration of hormonal signaling networks and mobile microRNAs is required for vascular patterning in *Arabidopsis* roots. Proc. Natl. Acad. Sci. USA **111**: 857–862.

Nordstrom, A., Tarkowski, P., Tarkowska, D., Norbaek, R., Åstot, C., Dolezal, K., Sandberg, G. (2004). Auxin regulation of cytokinin biosynthesis in *Arabidopsis* thaliana: a factor of potential importance for auxin–cytokinin-regulated development. Proc. Natl. Acad. Sci. USA **101**: 8039–8044.

Omelyanchuk, N.A., Kovrizhnykh, V.V., Oshchepkova, E.A., Pasternak, T., Palme, K., Mironova, V.V. (2016). A detailed expression map of the PIN1 auxin transporter in *Arabidopsis* thaliana root. BMC Plant Biol. **16**: 5.

Perilli, S., Di Mambro, R., Sabatini, S. (2012). Growth and development of the root apical meristem. Curr. Opin. Plant Biol. **15**:17–23.

Petersson, S.V., Johansson, A.I., Kowalczyk, M., Makoveychuk, A., Wang, J.Y., Moritz, T., Grebe, M., Benfey, P.N., Sandberg, G., Ljung, K. (2009). An auxin gradient and maximum in the *Arabidopsis* root apex shown by high-resolution cell-specific analysis of IAA distribution and synthesis. Plant Cell **21**: 1659–1668.

Petrasek, J. Friml J. (2009) Auxin transport routes in plant development. Development, 136, 2675-2688

Roychoudhry, S., Kepinski, S. (2022). Auxin in root development. Cold Spring Harb. Perspect. Biol. **14**: a039933.

Rutten, J., van den Berg, T., ten Tusscher, K. (2022). Modeling auxin signalling in roots: auxin computations. Cold Spring Harb. Perspect. Biol. **14**:.a040089.

Santner, A., Estelle, M. (2009). Recent advances and emerging trends in plant hormone signalling. Nature **459**: 1071-1078

Schaller, G.E., Bishopp, A., Kieber, J.J. 2(015). The yin-yang of hormones: cytokinin and auxin interactions in plant development. Plant Cell **27**: 44–63.

Shi, Y., Tian, S., Hou, L., Huang, X., Zhang, X., Guo, H., Yanga, S. (2012). Ethylene signaling negatively regulates freezing tolerance by repressing expression of CBF and Type-A ARR genes in *Arabidopsis*. Plant Cell **24**: 2578–2595.

Skoog, F., Miller, C.O. (1957). Chemical regulation of growth and organ formation in plant tissue cultured in vitro. Symp. Soc. Exp. Biol. **11**: 118-30.

To, J.P.C., Derue, J., Maxwell, B.B., Morris, V.F., Hutchison, C.E., Ferreira, F.J., Schaller, G.E., Kieber, J.J. (2007). Cytokinin regulates Type-A *Arabidopsis* Response Regulator activity and protein stability via two-component phosphorelay. Plant Cell **19**: 3901-3914.

Journal Pre-proof

Ursache, R., Grube Andersen, T., Marhavý, P., Geldner, N. (2018). A protocol for combining fluorescent proteins with histological stains for diverse cell wall components. Plant J. **93**: 399-412.

Vanstraelen, M., Benkova, E. (2012). Hormonal interactions in the regulation of plant development. Annu. Rev. Cell Devel. Biol. **28**: 463–487.

Vogel, J.P., Woeste, K.E., Theologis, A., Kieber, J.J. (1998). Recessive and dominant mutations in the ethylene biosynthetic gene ACS5 of *Arabidopsis* confer cytokinin insensitivity and ethylene overproduction, respectively. Proc. Natl. Acad. Sci. USA **95**: 4766–4771.

Weijers, D., Wagner, D. (2016). Transcriptional responses to the auxin hormone. Ann. Rev. Plant Biol. **67**: 21.1–21.36

Werner, T., Motyka, V., Laucou, V., Stems, R., Van Onckelen, H., Schmulling, T. (2003). Cytokinin deficient transgenic *Arabidopsis* plant show multiple developmental alterations indicating opposite function of cytokinins in the regulation of shoot and root meristem activity. Plant Cell **15**: 2532–2550

Werner, T., Kollmer, I., Bartrina, I., Holst, K., Schmulling, T. (2006). New insights into the biology of cytokinin degradation. Plant Biol. **8**: 371–381

Zhao, Y. (2010). Auxin biosynthesis and its role in plant development. Annu. Rev. Plant Biol. **61**: 49–64.

Zhao, Y. (2014). Auxin biosynthesis. The *Arabidopsis* Book **12**: e0173, doi/10.1199/tab.0173.

Zürcher, E., Tavor-Deslex, D., Lituiev, D,, Enkerli, K., Tarr, P.T., Müller, B. (2013). A robust and sensitive synthetic sensor to monitor the transcriptional output of the cytokinin signaling network in planta. Plant Physiol. **161**: 1066–1075

Journal Pre-proof

Figure Legends

Figure 1. An integrative mechanism for simultaneous auxin and cytokinin patterning in the *Arabidopsis* root development.
Auxin metabolism in each cell is regulated by ethylene and cytokinin signalling. Auxin transport within a cell is due to diffusion and its transport between cells is predominantly facilitated by the functions of PIN and AUX1 transporters. Cytokinin metabolism is regulated by auxin and ethylene, and it transports via diffusion. Ethylene metabolism is regulated by auxin and cytokinin, and it transports via diffusion. The POLARIS protein regulates ethylene signalling by interacting with its receptors. The mechanism integrates metabolism and transport of auxin, cytokinin and ethylene into an integrative system, and the patterning of the three hormones is regulated mutually. A. Detailed network for mutual regulation of auxin, cytokinin and ethylene, and the network is extracted from the more comprehensive network in Liu et al. (2017). B. Schematic description about mutual regulation between auxin, cytokinin and ethylene. This is a simplified summary of the detailed network (Figure 1A) with the red lines highlighting links based on additional biological evidence that is anaysed in detail in this research. → indicates activation; -l indicates inhibition. Connections marked using red-coloured lines in B highlight the novel regulatory relationships explored in this research. Connections marked using black-coloured lines in B are the regulatory relationships previously examined (Moore et al. 2015; 2017, Liu et al. 2017). All connections are based on either experimental data in our lab or established biological evidence in the literature. Auxin, auxin hormone; ET, ethylene; CK, cytokinin; PINm, PIN mRNA; PINp, PIN protein; PLSm, POLARIS mRNA; PLSp, POLARIS protein; X, downstream ethylene signalling; Ra*, active form of auxin receptor; Ra, inactive form of auxin receptor; Re*, active form of ethylene receptor, ETR1. Re, inactive form of ethylene receptor, ETR1; CTR1*, active form of CTR1; CTR1, inactive form of CTR1.

Figure 2. Relationship of auxin, cytokinin and ethylene in a homogenous cell.
A. Effects of changing auxin biosynthesis rate on auxin, cytokinin and ethylene concentration. B. Effects of changing cytokinin biosynthesis rate on auxin, cytokinin and ethylene concentration. C. Effects of changing ethylene biosynthesis rate on auxin, cytokinin and ethylene concentration.

Figure 3. Modelled auxin concentration patterning.

Journal Pre-proof

Modelled auxin patterning (A, C-F) is in good agreement with both IAA concentration distribution measured experimentally (Figure S2A; Figure 3 in Petersson et al. 2009) and auxin response patterning shown as DR5::GFP fluorescence (B). Approximately, along longitudinal direction, meristem is at the position of 200 μm to 650 μm; transition zone (TZ) is at the position of 650 μm to 750 μm and elongation zone is at the position of 750 μm to 1200 μm. Equations and parameter values are included in Table S1, S2 and S3.

Figure 4. Modelled cytokinin concentration patterning.

Modelled cytokinin concentration patterning (A, C-F) is in good agreement with both cytokinin concentration distribution measured experimentally (Figure S3A; Figure 5 in Antoniadi et al. 2015) and cytokinin response patterning shown as ARR5::GFP fluorescence (B). Equations and parameter values are included in Table S1.

Figure 5. Spatiotemporal modelling predicts auxin concentration, patterning and biosynthesis rate of various experimental observations as reported in the literature.

A. Auxin response distribution along cell position from the initials in different cell types (Similar to Figure S4; Supplementary Figure 6 in Liao et al. 2015). B. Minimum auxin response distribution in transition zone (similar to Figure S5; Figure 3 in Di Mambro et al. 2017). C. Average auxin concentration in different mutants (similar to Figure S6; Figure 4C in Chilley et al. 2006). D. Auxin biosynthesis rate distribution (similar to Figure S7; Figure 5 in Petersson et al. 2009). Meristem is at the position of ca. 200 μm to 650 μm; transition zone (TZ) is at the position of 650 μm to 750 μm; and elongation zone is at the position of 750 μm to 1200 μm, in the longitudial axis.

Figure 6. Spatiotemporal modelling predicts changes in PIN1 and PIN2 level and patterning in various mutants.

A. Modelled PIN1 and PIN2 level change in various mutants (Similar to Figure S8; Figure 1B in Liu et al. 2013); B. Modelled PIN1 and PIN2 patterning change in *pin3*, *pin4* and *pin7* single mutants (similar to Figure S9A; PIN1 patterning change in Figure 6 in Omelyanchuk et al. 2016) and modelled PIN1 and PIN2 patterning change in *pin3,4,7* triple mutants (similar to Figure S9B; PIN2 patterning change in Figure 1 in Blilou et al. 2005). C. Enlargement of *pin4* mutant in Figure 6B.

Figure 7. Modelled change in cytokinin concentration and patterning in *pls* mutant predicts experimental observation.

A. Modelled PLS protein distribution (right panel in A) and measured PLS GFP fluorescence (left pane in A). The actual concentration of PLS protein has not been experimentally

Journal Pre-proof

quantified, and therefore the colour of the experimental image indicates the relative change in the level of PLS protein. B. Modelled change in cytokinin concentration in the *pls* mutant relative to wildtype (similar to Table 1 in Liu et al. 2010). C. Modelled change in cytokinin concentration in *pls* mutant; D. TCSn:GFP fluorescence in wild type and *pls* mutant.

Supplementary Information

Figure S1. An example of simultaneously enhancing the concentration of auxin, cytokinin and ethylene by increasing auxin biosynthesis rate in homogenous cells of the root.

Figure S2. Experimental observations about auxin.

Figure S3. Experimental observations about cytokinin.

Figure S4. Experimental observations about auxin response trends in cell files above the initials and comparison between experimental observations and modelled results.

Figure S5. Experimental observations about auxin response minimum in the transition zone and comparison between experimental observations and modelled results.

Figure S6. Experimental observations about average auxin concentration trends in WT, *pls* mutant, pls etr1 double mutant, and PLSox and comparison between experimental observations and modelled results.

Figure S7. Experimental observations about patterning the rate of auxin biosynthesis.

Figure S8. Experimental observations about the average concentration trend of PIN1 and PIN2 proteins in WT, PLSox transgenic, *pls* and *etr1* mutants, and *pls etr1* double mutant.

Figure S9. Experimental observations about changes in PIN1 and PIN2 concentrations in *pin3*, *pin4*, *pin7* mutants.

Figure S10. Modelled ethylene concentration in wild type and the *pls* mutant.

Figure S11. Modelling reveals that auxin patterning still emerges when auxin biosynthesis is not regulated by cytokinin or ethylene (k2a=0) with all auxin transporters being fixed as those in the wildtype.

Figure S12. Same as Figure 5 in the main text, but in the absence of auxin biosynthesis regulation (k2a=0).

Journal Pre-proof

Figure S13. Same as Figure 6 in the main text, but in the absence of auxin biosynthesis regulation (k2a=0).

Figure S14. Same as Figure 7 in the main text, but in the absence of auxin biosynthesis regulation (k2a=0).

Figure S15. Same as Figure 5 in the main text, but in the absence of the regulation of cytokinin degradation by ethylene signalling (k19a=0).

Figure S16. Same as Figure 6 in the main text, but in the absence of the regulation of cytokinin degradation by ethylene signalling (k19a=0).

Figure S17. Same as Figure 7 in the main text, but in the absence of the regulation of cytokinin degradation by ethylene signalling (k19a=0).

Figure S18. Same as Figure 5 in the main text, but in the absence of the regulation of cytokinin biosynthesis by auxin signalling (k18a=0).

Figure **S19**. Same as Figure 6 in the main text, but in the absence of the regulation of cytokinin biosynthesis by auxin signalling (k18a=0).

Figure S20. Same as Figure 7 in the main text, but in the absence of the regulation of cytokinin biosynthesis by auxin signalling (k18a=0).

Figure S21. Role of changes in PIN1 and PIN2 concentration and patterning in *pin3* mutant.

Figure S22. Role of changes in PIN1 and PIN2 concentration and patterning in *pin4* mutant.

Figure S23. Role of changes in PIN1 and PIN2 concentration and patterning in *pin7* mutant.

Figure S24. Role of changes in PIN1 and PIN2 concentration and patterning in *pin3,4,7* triple mutant.

Figure S25. Role of PLS over expressor in the concentration and patterning of auxin, cytokinin and ethylene.

Figure S26. Role of *ctr1* mutant in the concentration and patterning of auxin, cytokinin and ethylene.

Figure S27. Role of decreasing CTR1 downstream response in the concentration and patterning of auxin, cytokinin and ethylene.

Journal Pre-proof

Figure S28. Role of increasing CTR1 downstream response in the concentration and patterning of auxin, cytokinin and ethylene.

Figure S29. Schematic summary of the complex multi–level regulatory relationships for simultaneous auxin and cytokinin concentration patterning in the root.

Table S1. Hormonal crosstalk rate equations and parameter values for species biosynthesis, decay, activation and inactivation at each grid point.

Table S2. PIN1 and PIN2 rate equations for localisation to and from the plasma membrane.

Table S3. Species flux between nearest neighbour.

Journal Pre-proof

A

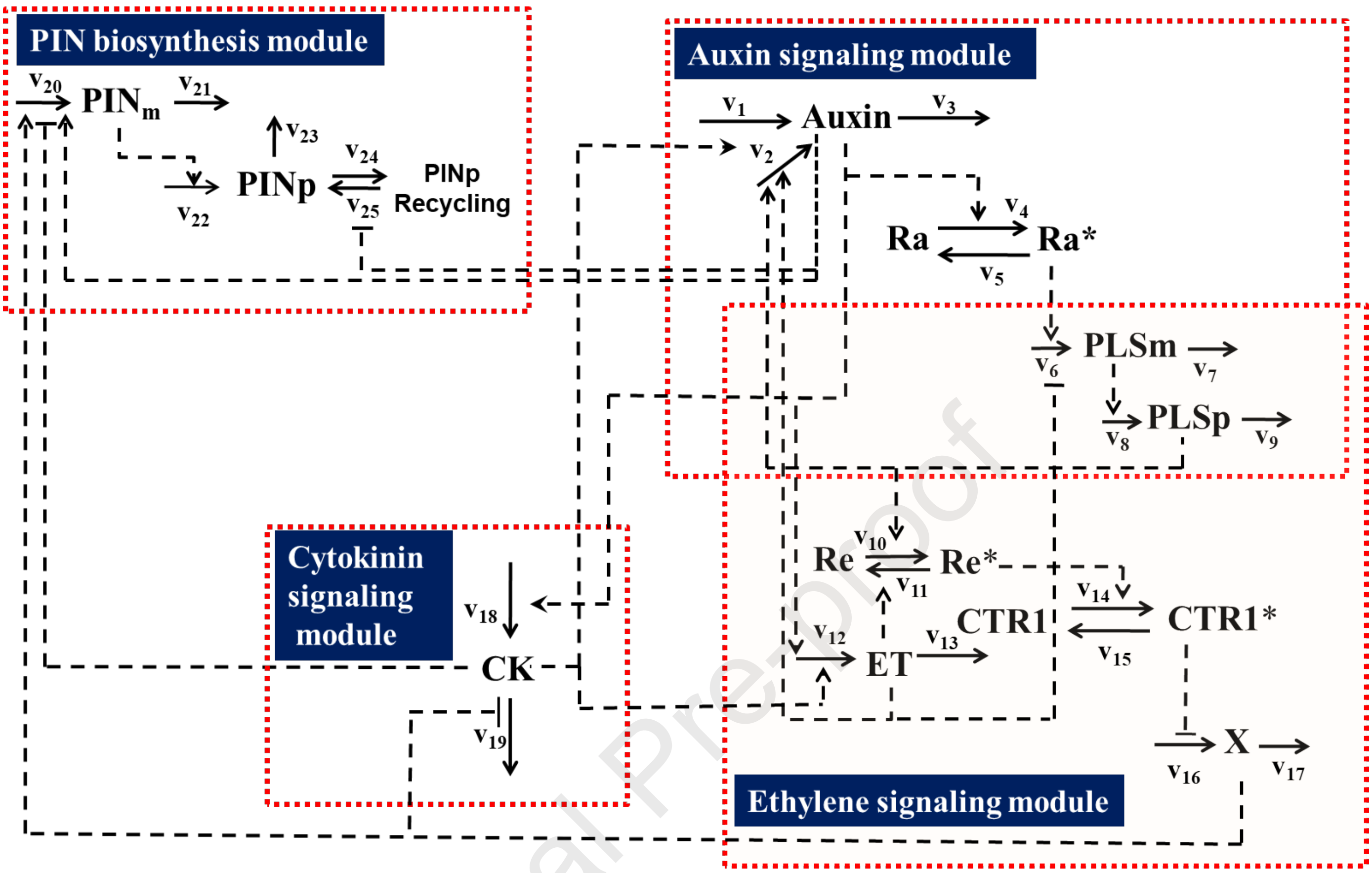

B

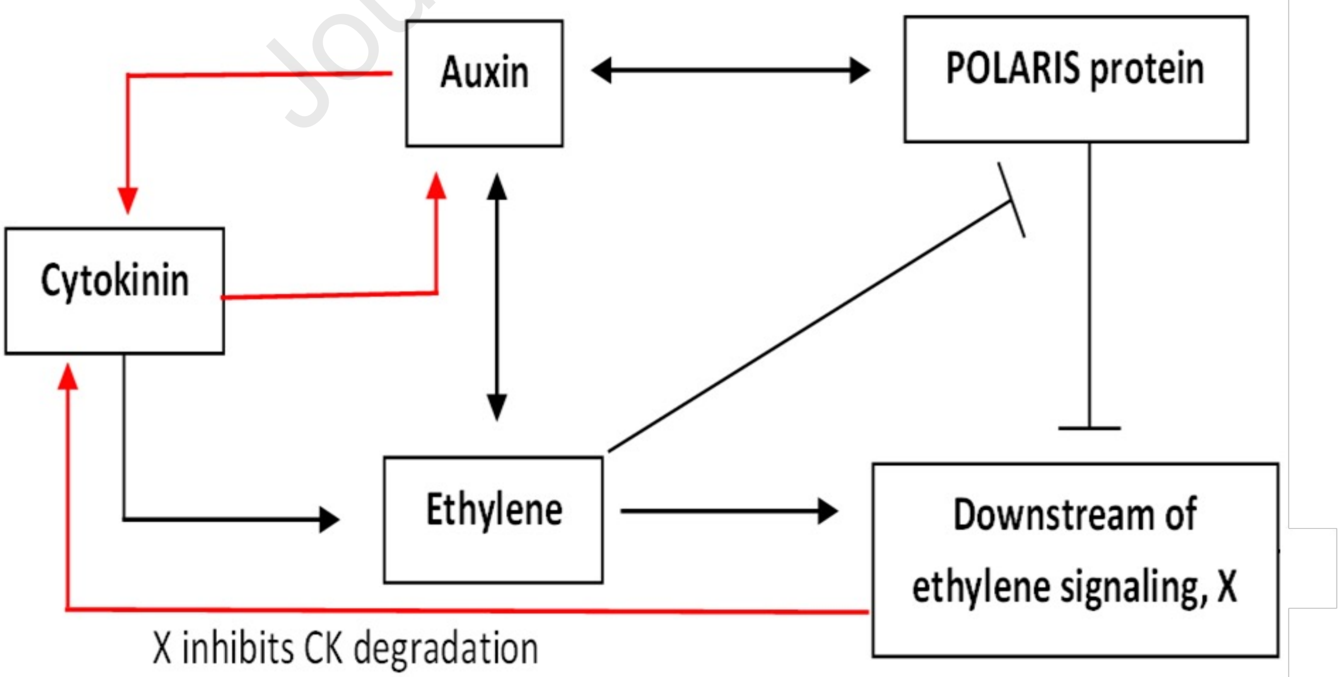

Journal Pre-proof

Figure 1. An integrative mechanism for simultaneous auxin and cytokinin patterning in the *Arabidopsis* root development.

Auxin metabolism in each cell is regulated by ethylene and cytokinin signalling. Auxin transport within a cell is due to diffusion and its transport between cells is predominantly facilitated by the functions of PIN and AUX1 transporters. Cytokinin metabolism is regulated by auxin and ethylene, and it transports via diffusion. Ethylene metabolism is regulated by auxin and cytokinin, and it transports via diffusion. The POLARIS protein regulates ethylene signalling by interacting with its receptors. The mechanism integrates metabolism and transport of auxin, cytokinin and ethylene into an integrative system, and the patterning of the three hormones is regulated mutually. A. Detailed network for mutual regulation of auxin, cytokinin and ethylene, and the network is extracted from the more comprehensive network in Liu et al. (2017). B. Schematic description about mutual regulation between auxin, cytokinin and ethylene. This is a simplified summary of the detailed network (Figure 1A) with the red lines highlighting links based on additional biological evidence that is anaysed in detail in this research. → indicates activation; -I indicates inhibition. Connections marked using red-coloured lines in B highlight the novel regulatory relationships explored in this research. Connections marked using black-coloured lines in B are the regulatory relationships previously examined (Moore et al. 2015; 2017, Liu et al. 2017). All connections are based on either experimental data in our lab or established biological evidence in the literature. Auxin, auxin hormone; ET, ethylene; CK, cytokinin; PINm, PIN mRNA; PINp, PIN protein; PLSm, POLARIS mRNA; PLSp, POLARIS protein; X, downstream ethylene signalling; Ra*, active form of auxin receptor; Ra, inactive form of auxin receptor; Re*, active form of ethylene receptor, ETR1. Re, inactive form of ethylene receptor, ETR1; CTR1*, active form of CTR1; CTR1, inactive form of CTR1.

Journal Pre-proof

Journal Pre-proof

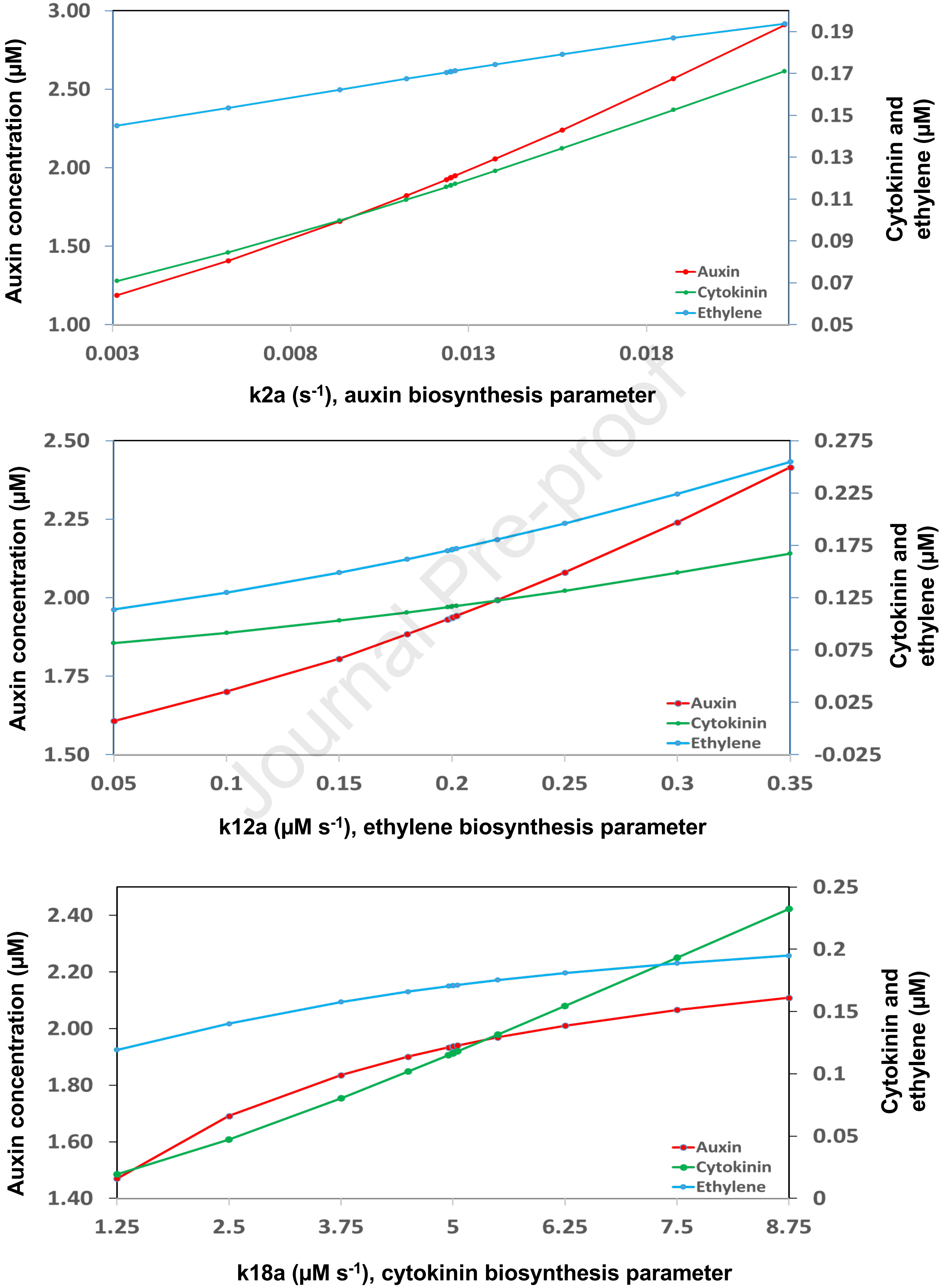

Journal Pre-proof

Figure 2. Relationship of auxin, cytokinin and ethylene in a homogenous cell.

A. Effects of changing auxin biosynthesis rate on auxin, cytokinin and ethylene concentration. B. Effects of changing cytokinin biosynthesis rate on auxin, cytokinin and ethylene concentration. C. Effects of changing ethylene biosynthesis rate on auxin, cytokinin and ethylene concentration.

Journal Pre-proof

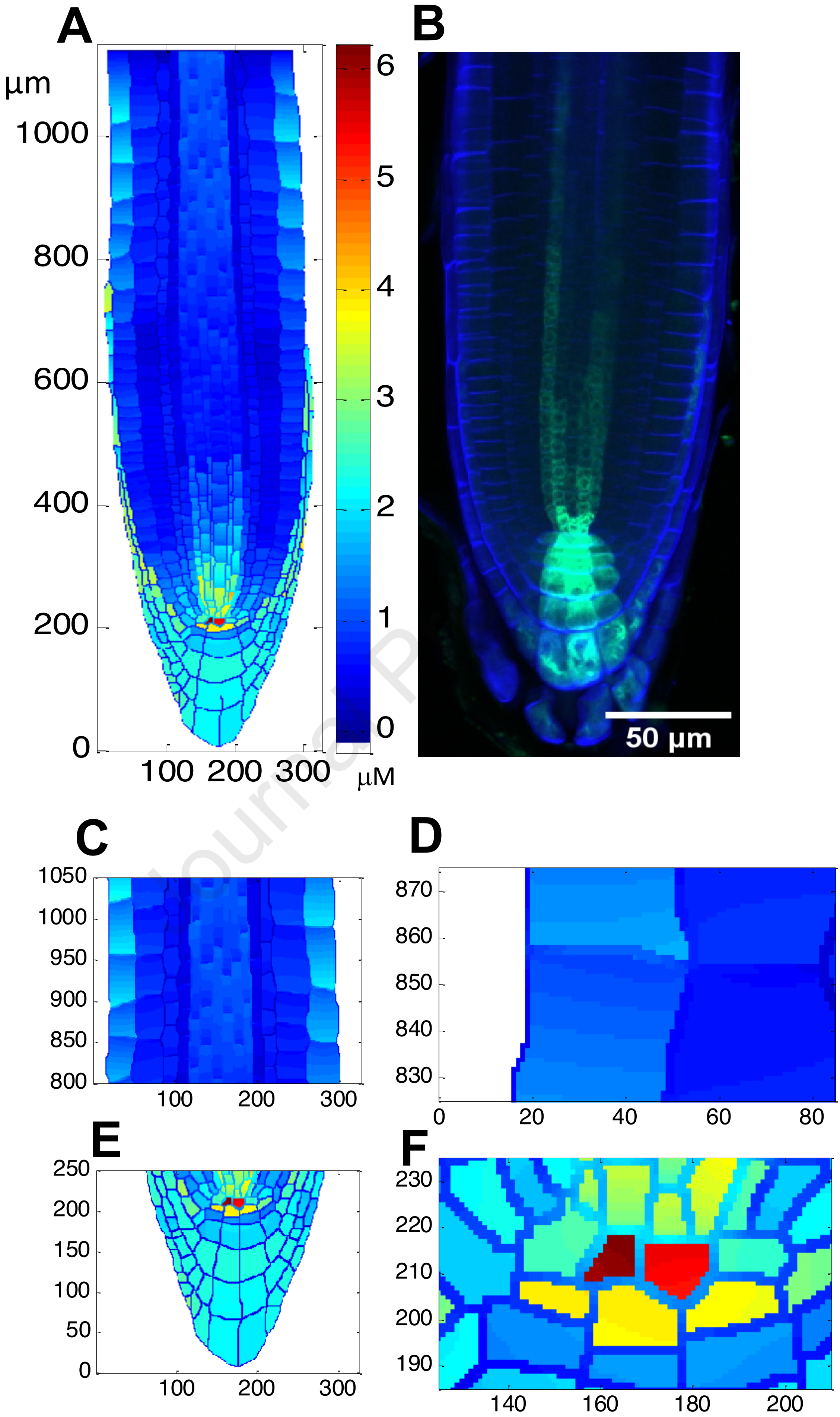
A
µm
1000
800
600
400
200
0
100 200 300
6
5
4
3
2
1
0
µM
B
50 µm
C
1050
1000
950
900
850
800
100
200
300
D
870
860
850
840
830
0
20
40
60
80
E
250
200
150
100
50
0
100
200
300
F
230
220
210
200
190
140
160
180
200

Figure 3. Modelled auxin concentration patterning.

Modelled auxin patterning (A, C-F) is in good agreement with both IAA concentration distribution measured experimentally (Figure S2A; Figure 3 in Petersson et al. 2009) and auxin response patterning shown as DR5::GFP fluorescence (B). Approximately, along longitudinal direction, meristem is at the position of 200 μm to 650 μm; transition zone (TZ) is at the position of 650 μm to 750 μm and elongation zone is at the position of 750 μm to 1200 μm. Equations and parameter values are included in Table S1, S2 and S3.

Journal Pre-proof

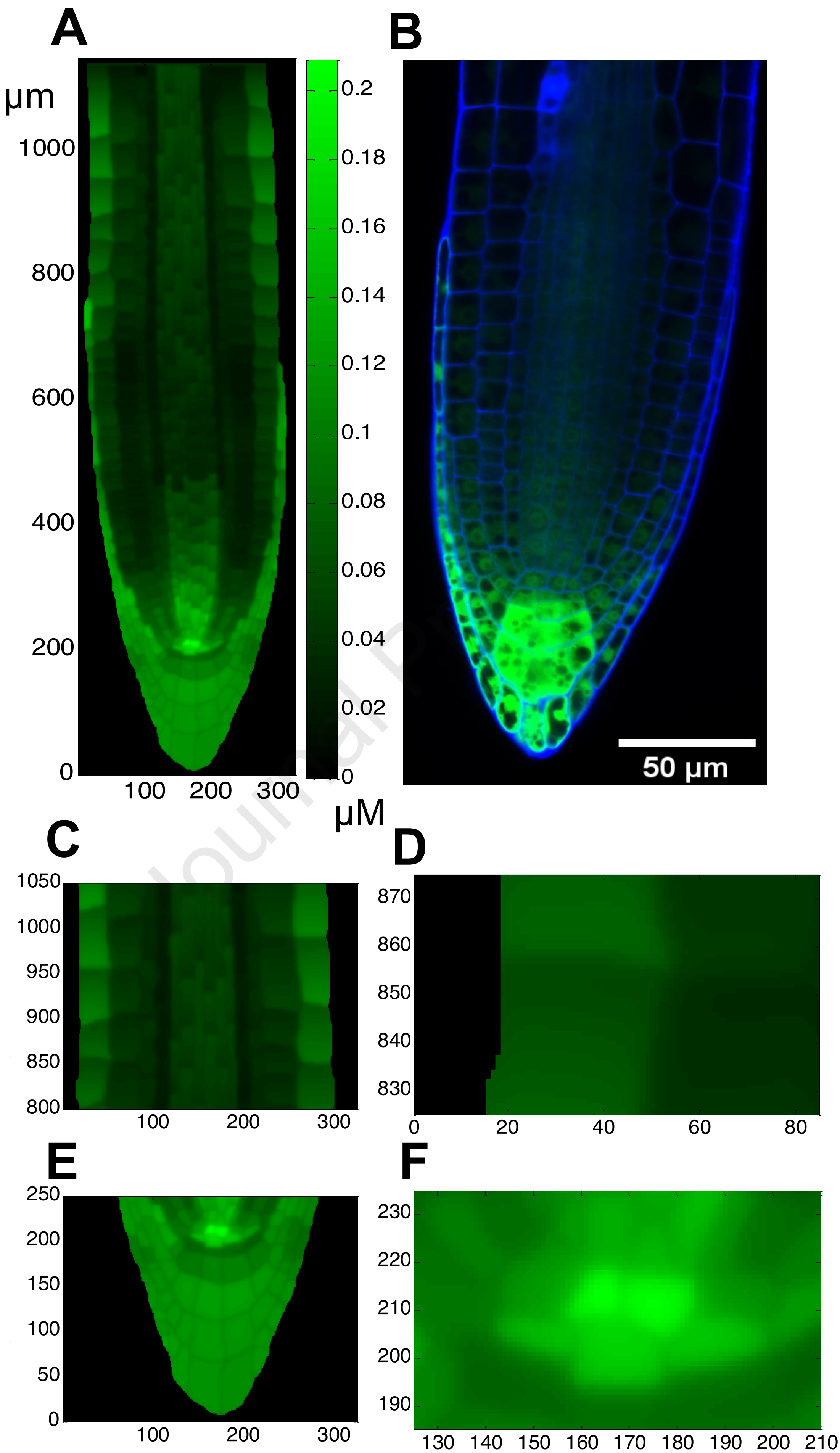
A
μm
1000
800
600
400
200
0
100 200 300
0.2
0.18
0.16
0.14
0.12
0.1
0.08
0.06
0.04
0.02
0
μM
B
50 μm
C
1050
1000
950
900
850
800
100 200 300
D
870
860
850
840
830
0 20 40 60 80
E
250
200
150
100
50
0
100 200 300
F
230
220
210
200
190
130 140 150 160 170 180 190 200 210

Figure 4. Modelled cytokinin concentration patterning.

Modelled cytokinin concentration patterning (A, C-F) is in good agreement with both cytokinin concentration distribution measured experimentally (Figure S3A; Figure 5 in Antoniadi et al. 2015) and cytokinin response patterning shown as ARR5::GFP fluorescence (B). Equations and parameter values are included in Table S1.

Journal Pre-proof

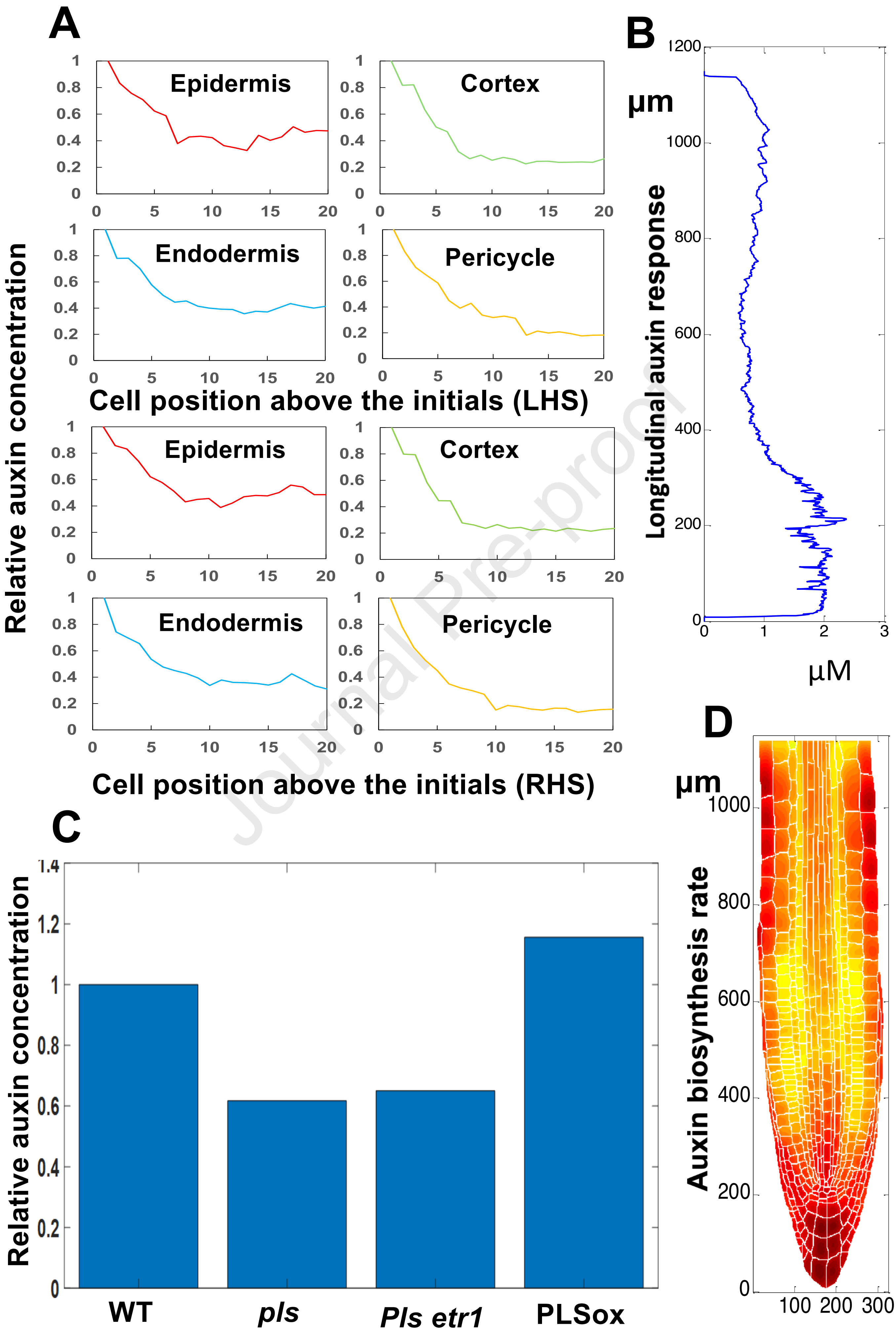

Journal Pre-proof

Figure 5. Spatiotemporal modelling predicts auxin concentration, patterning and biosynthesis rate of various experimental observations as reported in the literature.

A. Auxin response distribution along cell position from the initials in different cell types (Similar to Figure S4; Supplementary Figure 6 in Liao et al. 2015). B. Minimum auxin response distribution in transition zone (similar to Figure S5; Figure 3 in Di Mambro et al. 2017). C. Average auxin concentration in different mutants (similar to Figure S6; Figure 4C in Chilley et al. 2006). D. Auxin biosynthesis rate distribution (similar to Figure S7; Figure 5 in Petersson et al. 2009). Meristem is at the position of ca. 200 μm to 650 μm; transition zone (TZ) is at the position of 650 μm to 750 μm; and elongation zone is at the position of 750 μm to 1200 μm, in the longitudial axis.

Journal Pre-proof

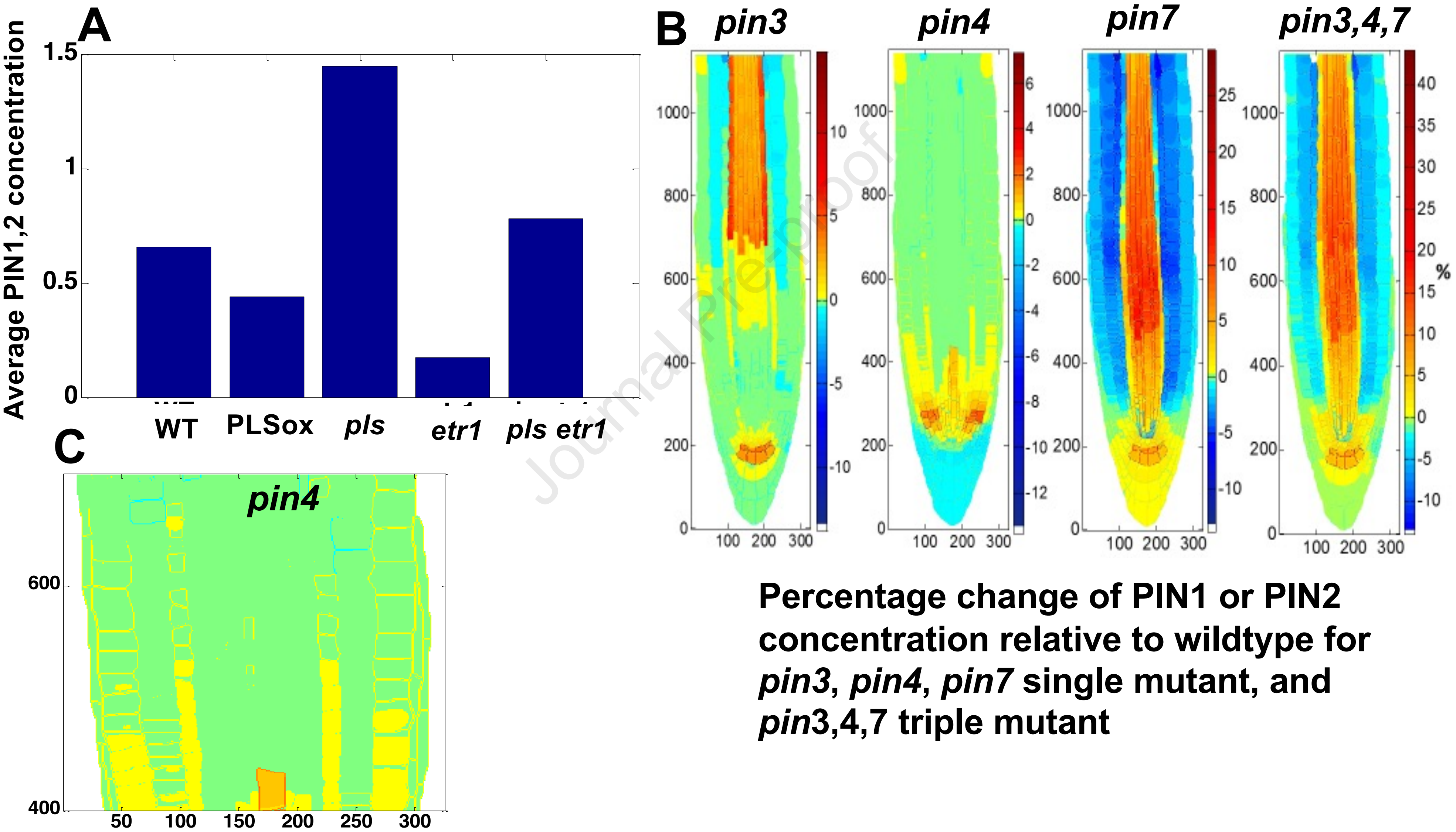

Percentage change of PIN1 or PIN2 concentration relative to wildtype for *pin3*, *pin4*, *pin7* single mutant, and *pin*3,4,7 triple mutant

Journal Pre-proof

Figure 6. Spatiotemporal modelling predicts changes in PIN1 and PIN2 level and patterning in various mutants.

A. Modelled PIN1 and PIN2 level change in various mutants (Similar to Figure S8; Figure 1B in Liu et al. 2013); B. Modelled PIN1 and PIN2 patterning change in *pin3*, *pin4* and *pin7* single mutants (similar to Figure S9A; PIN1 patterning change in Figure 6 in Omelyanchuk et al. 2016) and modelled PIN1 and PIN2 patterning change in *pin3,4,7* triple mutants (similar to Figure S9B; PIN2 patterning change in Figure 1 in Blilou et al. 2005). C. Enlargement of *pin4* mutant in Figure 6B.

Journal Pre-proof

Journal Pre-proof

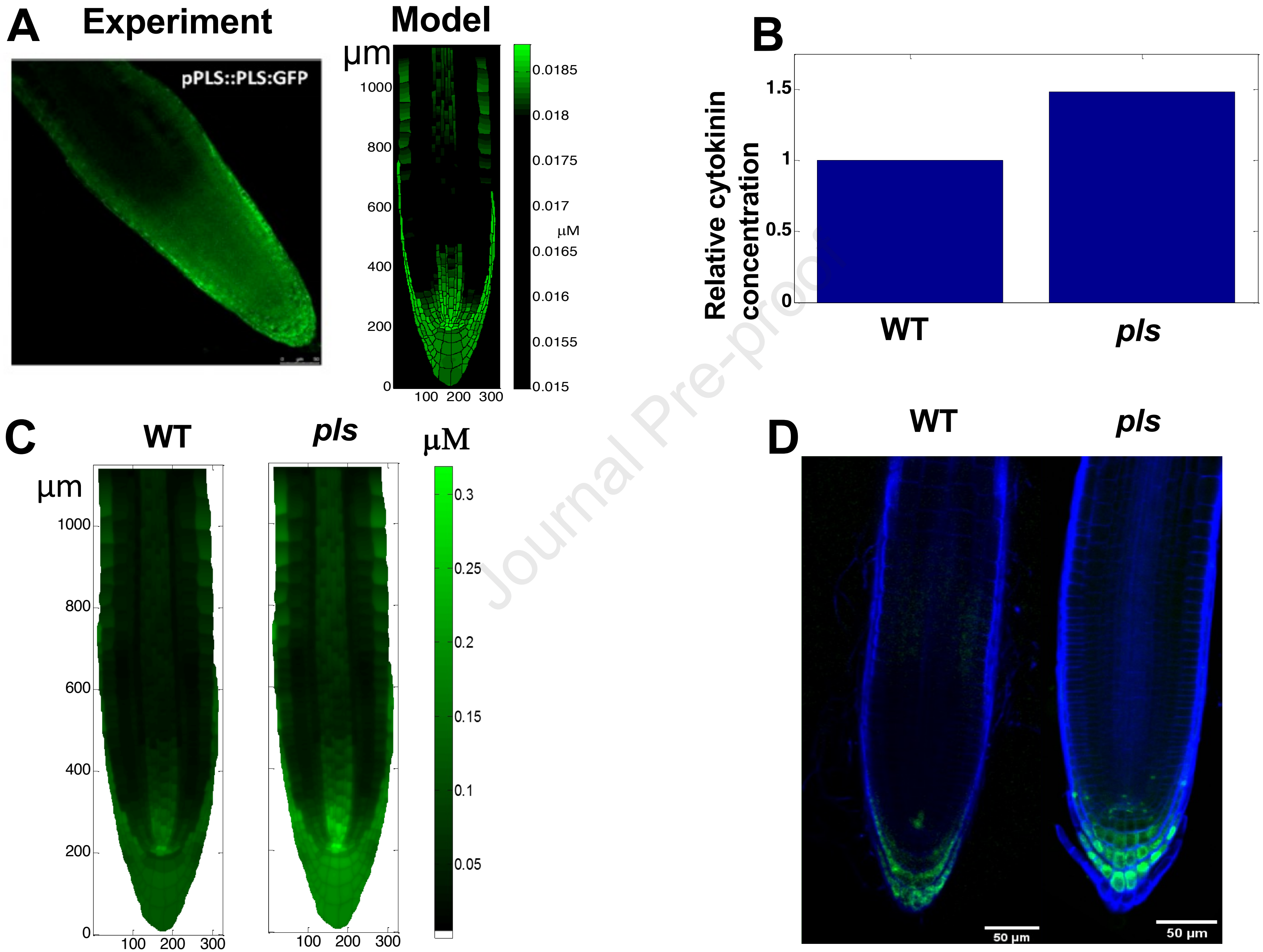

Journal Pre-proof

Figure 7. Modelled change in cytokinin concentration and patterning in *pls* mutant predicts experimental observation.

A. Modelled PLS protein distribution (right panel in A) and measured PLS GFP fluorescence (left pane in A). The actual concentration of PLS protein has not been experimentally quantified, and therefore the colour of the experimental image indicates the relative change in the level of PLS protein. B. Modelled change in cytokinin concentration in the *pls* mutant relative to wildtype (similar to Table 1 in Liu et al. 2010). C. Modelled change in cytokinin concentration in *pls* mutant; D. TCSn:GFP fluorescence in wild type and *pls* mutant.

Journal Pre-proof